

World Journal of *Gastroenterology*

World J Gastroenterol 2024 February 28; 30(8): 779-993



EDITORIAL

- 779 Immunotherapy of gastric cancer: Present status and future perspectives
Triantafyllidis JK, Konstadoulakis MM, Papalois AE
- 794 Immune signature of small bowel adenocarcinoma and the role of tumor microenvironment
Christodoulidis G, Kouliou MN, Koumarelas KE
- 799 Management of autoimmune hepatitis induced by hepatitis delta virus
Gigi E, Lagopoulos V, Liakos A
- 806 Adjuvant therapy for hepatocellular carcinoma: Dilemmas at the start of a new era
Zhong JH

OPINION REVIEW

- 811 Nonsteroidal anti-inflammatory drugs before endoscopic ultrasound guided tissue acquisition to reduce the incidence of post procedural pancreatitis
de Jong M, van Delft F, Roozen C, van Geenen EJ, Bisseling T, Siersema P, Bruno M

REVIEW

- 817 Autoimmune pancreatitis: Cornerstones and future perspectives
Gallo C, Dispinzieri G, Zucchini N, Invernizzi P, Massironi S

MINIREVIEWS

- 833 Fecal microbiota transplantation for treatment of non-alcoholic fatty liver disease: Mechanism, clinical evidence, and prospect
Qiu XX, Cheng SL, Liu YH, Li Y, Zhang R, Li NN, Li Z

ORIGINAL ARTICLE**Retrospective Study**

- 843 Transcatheter arterial chemoembolization combined with PD-1 inhibitors and Lenvatinib for hepatocellular carcinoma with portal vein tumor thrombus
Wu HX, Ding XY, Xu YW, Yu MH, Li XM, Deng N, Chen JL
- 855 Immunoglobulin G-mediated food intolerance and metabolic syndrome influence the occurrence of reflux esophagitis in *Helicobacter pylori*-infected patients
Wang LH, Su BB, Wang SS, Sun GC, Lv KM, Li Y, Shi H, Chen QQ
- 863 Evaluating the influence of sarcopenia and myosteatosis on clinical outcomes in gastric cancer patients undergoing immune checkpoint inhibitor
Deng GM, Song HB, Du ZZ, Xue YW, Song HJ, Li YZ

Observational Study

- 881 Mitochondrial dysfunction affects hepatic immune and metabolic remodeling in patients with hepatitis B virus-related acute-on-chronic liver failure
Zhang Y, Tian XL, Li JQ, Wu DS, Li Q, Chen B

Basic Study

- 901 Metadherin promotes stem cell phenotypes and correlated with immune infiltration in hepatocellular carcinoma
Wang YY, Shen MM, Gao J
- 919 Lipid metabolism-related long noncoding RNA RP11-817I4.1 promotes fatty acid synthesis and tumor progression in hepatocellular carcinoma
Wang RY, Yang JL, Xu N, Xu J, Yang SH, Liang DM, Li JZ, Zhu H

SYSTEMATIC REVIEWS

- 943 Quality of life after pancreatic surgery
Li SZ, Zhen TT, Wu Y, Wang M, Qin TT, Zhang H, Qin RY

META-ANALYSIS

- 956 Prevalence and clinical impact of sarcopenia in liver transplant recipients: A meta-analysis
Jiang MJ, Wu MC, Duan ZH, Wu J, Xu XT, Li J, Meng QH

SCIENTOMETRICS

- 969 Bibliometrics analysis based on the Web of Science: Current trends and perspective of gastric organoid during 2010-2023
Jiang KL, Jia YB, Liu XJ, Jia QL, Guo LK, Wang XX, Yang KM, Wu CH, Liang BB, Ling JH

CASE REPORT

- 984 Cronkhite-Canada syndrome with esophagus involvement and six-year follow-up: A case report
Tang YC

LETTER TO THE EDITOR

- 991 Monitoring of hepatocellular carcinoma
Akkari I, Jaziri H

ABOUT COVER

Editorial Board Member of *World Journal of Gastroenterology*, Neal Shahidi, MD, FRCPC, PhD, Assistant Professor, Department of Medicine, Division of Gastroenterology, St Paul's Hospital, Vancouver V6Z 2K5, British Columbia, Canada. nshahidi@providencehealth.bc.ca

AIMS AND SCOPE

The primary aim of *World Journal of Gastroenterology* (*WJG*, *World J Gastroenterol*) is to provide scholars and readers from various fields of gastroenterology and hepatology with a platform to publish high-quality basic and clinical research articles and communicate their research findings online. *WJG* mainly publishes articles reporting research results and findings obtained in the field of gastroenterology and hepatology and covering a wide range of topics including gastroenterology, hepatology, gastrointestinal endoscopy, gastrointestinal surgery, gastrointestinal oncology, and pediatric gastroenterology.

INDEXING/ABSTRACTING

The *WJG* is now abstracted and indexed in Science Citation Index Expanded (SCIE), MEDLINE, PubMed, PubMed Central, Scopus, Reference Citation Analysis, China Science and Technology Journal Database, and Superstar Journals Database. The 2023 edition of Journal Citation Reports® cites the 2022 impact factor (IF) for *WJG* as 4.3; Quartile category: Q2. The *WJG*'s CiteScore for 2021 is 8.3.

RESPONSIBLE EDITORS FOR THIS ISSUE

Production Editor: *Yu-Xi Chen*; Production Department Director: *Xiang Li*; Editorial Office Director: *Jia-Ru Fan*.

NAME OF JOURNAL

World Journal of Gastroenterology

ISSN

ISSN 1007-9327 (print) ISSN 2219-2840 (online)

LAUNCH DATE

October 1, 1995

FREQUENCY

Weekly

EDITORS-IN-CHIEF

Andrzej S Tarnawski

EXECUTIVE ASSOCIATE EDITORS-IN-CHIEF

EDITORIAL BOARD MEMBERS

<http://www.wjgnet.com/1007-9327/editorialboard.htm>

PUBLICATION DATE

February 28, 2024

COPYRIGHT

© 2024 Baishideng Publishing Group Inc

PUBLISHING PARTNER

Shanghai Pancreatic Cancer Institute and Pancreatic Cancer Institute, Fudan University
Biliary Tract Disease Institute, Fudan University

INSTRUCTIONS TO AUTHORS

<https://www.wjgnet.com/bpg/gerinfo/204>

GUIDELINES FOR ETHICS DOCUMENTS

<https://www.wjgnet.com/bpg/gerinfo/287>

GUIDELINES FOR NON-NATIVE SPEAKERS OF ENGLISH

<https://www.wjgnet.com/bpg/gerinfo/240>

PUBLICATION ETHICS

<https://www.wjgnet.com/bpg/gerinfo/288>

PUBLICATION MISCONDUCT

<https://www.wjgnet.com/bpg/gerinfo/208>

Xian-Jun Yu (Pancreatic Oncology), Jian-Gao Fan (Chronic Liver Disease), Hou-Bao Liu (Biliary Tract Disease)

ARTICLE PROCESSING CHARGE

<https://www.wjgnet.com/bpg/gerinfo/242>

STEPS FOR SUBMITTING MANUSCRIPTS

<https://www.wjgnet.com/bpg/gerinfo/239>

ONLINE SUBMISSION

<https://www.f6publishing.com>

PUBLISHING PARTNER'S OFFICIAL WEBSITE

<https://www.shca.org.cn>
<https://www.zs-hospital.sh.cn>

Observational Study

Mitochondrial dysfunction affects hepatic immune and metabolic remodeling in patients with hepatitis B virus-related acute-on-chronic liver failure

Yu Zhang, Xiao-Ling Tian, Jie-Qun Li, Dong-Sheng Wu, Qiang Li, Bin Chen

Specialty type: Gastroenterology and hepatology**Provenance and peer review:**

Unsolicited article; Externally peer reviewed.

Peer-review model: Single blind**Peer-review report's scientific quality classification**Grade A (Excellent): 0
Grade B (Very good): B
Grade C (Good): 0
Grade D (Fair): 0
Grade E (Poor): 0**P-Reviewer:** Venegas M, Chile**Received:** October 8, 2023**Peer-review started:** October 8, 2023**First decision:** December 8, 2023**Revised:** December 15, 2023**Accepted:** January 23, 2024**Article in press:** January 23, 2024**Published online:** February 28, 2024**Yu Zhang, Xiao-Ling Tian, Bin Chen**, Department of Hepatology, Institute of Hepatology, The First Affiliated Hospital of Hunan University of Chinese Medicine, Changsha 410021, Hunan Province, China**Jie-Qun Li, Qiang Li**, Department of Liver Transplant, Transplant Medical Research Center, The Second Xiangya Hospital of Central South University, Changsha 410011, Hunan Province, China**Dong-Sheng Wu**, Department of Surgery, The First Affiliated Hospital of Hunan University of Chinese Medicine, Changsha 410021, Hunan Province, China**Corresponding author:** Bin Chen, PhD, Chief Physician, Department of Hepatology, Institute of Hepatology, The First Affiliated Hospital of Hunan University of Chinese Medicine, No. 95 Middle Shaoshan Road, Yuhua District, Changsha 410021, Hunan Province, China.
chenbin0410@126.com**Abstract****BACKGROUND**

Immune dysregulation and metabolic derangement have been recognized as key factors that contribute to the progression of hepatitis B virus (HBV)-related acute-on-chronic liver failure (ACLF). However, the mechanisms underlying immune and metabolic derangement in patients with advanced HBV-ACLF are unclear.

AIM

To identify the bioenergetic alterations in the liver of patients with HBV-ACLF causing hepatic immune dysregulation and metabolic disorders.

METHODS

Liver samples were collected from 16 healthy donors (HDs) and 17 advanced HBV-ACLF patients who were eligible for liver transplantation. The mitochondrial ultrastructure, metabolic characteristics, and immune microenvironment of the liver were assessed. More focus was given to organic acid metabolism as well as the function and subpopulations of macrophages in patients with HBV-ACLF.

RESULTS

Compared with HDs, there was extensive hepatocyte necrosis, immune cell infiltr-

ration, and ductular reaction in patients with ACLF. In patients, the liver suffered severe hypoxia, as evidenced by increased expression of hypoxia-inducible factor-1 α . Swollen mitochondria and cristae were observed in the liver of patients. The number, length, width, and area of mitochondria were adaptively increased in hepatocytes. Targeted metabolomics analysis revealed that mitochondrial oxidative phosphorylation decreased, while anaerobic glycolysis was enhanced in patients with HBV-ACLF. These findings suggested that, to a greater extent, hepatocytes used the extra-mitochondrial glycolytic pathway as an energy source. Patients with HBV-ACLF had elevated levels of chemokine C-C motif ligand 2 in the liver homogenate, which stimulates peripheral monocyte infiltration into the liver. Characterization and functional analysis of macrophage subsets revealed that patients with ACLF had a high abundance of CD68⁺ HLA-DR⁺ macrophages and elevated levels of both interleukin-1 β and transforming growth factor- β 1 in their livers. The abundance of CD206⁺ CD163⁺ macrophages and expression of interleukin-10 decreased. The correlation analysis revealed that hepatic organic acid metabolites were closely associated with macrophage-derived cytokines/chemokines.

CONCLUSION

The results indicated that bioenergetic alteration driven by hypoxia and mitochondrial dysfunction affects hepatic immune and metabolic remodeling, leading to advanced HBV-ACLF. These findings highlight a new therapeutic target for improving the treatment of HBV-ACLF.

Key Words: Acute-on-chronic liver failure; Hypoxia-inducible factor-1 α ; Mitochondria; Metabolic phenotype; Immune cells

©The Author(s) 2024. Published by Baishideng Publishing Group Inc. All rights reserved.

Core Tip: Our data were obtained from liver of patients with hepatitis B virus (HBV)-related acute-on-chronic liver failure (ACLF), whose mitochondrial function, metabolites, and immune microenvironment were less susceptible to any confounding factors caused by other failing organs. Widely infiltrating macrophages were originated from peripheral circulating monocytes in the liver of patients with HBV-ACLF. Mitochondrial oxidative phosphorylation was decreased, and anaerobic glycolysis was enhanced in patients with HBV-ACLF. Liver of patients made greater use of the extra-mitochondrial glycolytic pathway for providing energy. Bioenergetic alteration driven by hypoxia and mitochondrial dysfunction contribute to hepatic immune and metabolic remodeling, may leading to organ failure and poor clinical prognosis in patients with advanced HBV-ACLF.

Citation: Zhang Y, Tian XL, Li JQ, Wu DS, Li Q, Chen B. Mitochondrial dysfunction affects hepatic immune and metabolic remodeling in patients with hepatitis B virus-related acute-on-chronic liver failure. *World J Gastroenterol* 2024; 30(8): 881-900

URL: <https://www.wjgnet.com/1007-9327/full/v30/i8/881.htm>

DOI: <https://dx.doi.org/10.3748/wjg.v30.i8.881>

INTRODUCTION

Acute-on-chronic liver failure (ACLF) is a syndrome characterized by acute decompensation of chronic liver disease associated with organ failure and high short-term mortality. Hepatitis B virus (HBV)-related ACLF is the most common type of liver failure in the Asia-Pacific region[1]. It is characterized by excessive immune response due to HBV reactivation. HBV-ACLF leads to acute hepatic decompensation in patients with chronic liver disease or cirrhosis[2]. The excessive immune response is caused by molecular patterns that are associated with bacterial pathogens and damage, which activate pattern recognition receptors of the innate immune system. The core immune mechanisms in HBV-ACLF involve the activation of the innate immune system and impaired adaptive immune response[2].

The interactions between HBV reactivation, immune dysregulation, and inflammatory response form an intricate network that lead the pathogenesis of ACLF. Each of these processes has a tremendous demand for energy and nutrients. Therefore, the liver needs to adjust its metabolic patterns to generate sufficient energy for supporting viral replication, inflammatory response, and immune cell activation. Dysregulation of this process causes metabolic disturbance and energy crisis, which might result in organ failure. Recent transcriptome and metabolomics studies have shown that there are significant changes in metabolic pathways, including lipid metabolism, fatty acid metabolism, and oxygen homeostasis, in all stages of HBV-ACLF[2]. Decreased oxidative phosphorylation and increased fatty acid β -oxidation were also observed in HBV-ACLF[3]. Mitochondria are the central hubs of energy production and metabolic processes that mainly regulate oxidative phosphorylation and produce ATP. Remodeling mitochondrial metabolism is essential for regulating innate immunity and inflammatory response. Mitochondrial dysfunction is a hallmark of ACLF, which controls the metabolism of leukocytes in patients with acute decompensated cirrhosis and ACLF[4]. Profound alterations in metabolic pathways have been observed in patients with HBV-ACLF. It has also been noted that mitochondrial dysfunction might reprogram energy metabolism in ACLF.

We hypothesized that mitochondrial structure and function are altered in patients with HBV-ACLF, causing a shift in cellular energy metabolism, metabolic patterns, and immune response in patients with ACLF. In this study, the tissue levels of organic acid metabolites and innate immune cells in patients with advanced HBV-ACLF were measured. The mitochondrial ultrastructure was assessed using transmission electron microscopy (TEM). Biomarkers of mitochondrial dysfunction were measured to monitor mitochondrial impairment.

MATERIALS AND METHODS

Patients

The study used liver tissue samples from 17 patients with HBV-ACLF (a group hereafter called “ACLF”) and 16 healthy donors (HDs) at The Second Xiangya Hospital of Central South University. Patients with HBV-ACLF met the diagnostic criteria for ACLF suggested by the China Medical Association[5]. Based on this criterion, reactivation of hepatitis B virus causes progressive acute jaundice and coagulation dysfunction, which can be accompanied by hepatic encephalopathy, ascites, electrolyte imbalance, infection, hepatorenal syndrome, and the hepatopulmonary syndrome. Other symptoms and complications, such as extrahepatic organ failure, may also exist. The jaundice rapidly progresses, with a serum total bilirubin (TBIL) $\geq 10 \times$ upper limit of normal or a daily increase of $\geq 17.1 \mu\text{mol/L}$. Hemorrhagic manifestations present with prothrombin time (PT) activity (PTA) $\leq 40\%$ [or international normalized ratio (INR) ≥ 1.5]. The inclusion criteria used in this study were as follows: (1) Patients with HBV-ACLF eligible for liver transplantation; (2) model for end-stage liver disease (MELD) score more than or equal to 15[5]; and (3) 18–70-year-old male or female. The exclusion criteria were as follows: (1) Super-infection or co-infection with other hepatotropic and non-hepatotropic viruses; (2) previous application of any immunomodulatory agents or cytotoxic/immunosuppressive drugs within the last three months; (3) hepatocellular carcinoma or extrahepatic malignancies; and (4) co-existence of other liver diseases, such as alcoholic liver disease, Wilson disease, drug-induced liver injury, or autoimmune hepatitis.

All liver tissues were obtained after liver transplantation. Donor livers were lavaged and trimmed before transplantation. The native liver tissues were collected after trimming, before they were washed with an ice-cold PBS solution. The study protocol was approved by the Ethics Committee of the First Hospital of Hunan University of Chinese Medicine (No. HN-LL-SWST-15), and written informed consent was obtained from all participants.

Clinical data collection

Demographic and laboratory data were collected, including age, gender, white blood cell (WBC), neutrophil count, platelet count (PLT), TBIL, aspartate transaminase (AST), alanine transaminase (ALT), albumin (ALB), creatinine, blood urea nitrogen, PT, INR, PTA, hypersensitive C-reactive protein (hs-CRP), procalcitonin (PCT), lactate (LAC), and erythrocyte sedimentation rate. ACLF risk scores were calculated. All laboratory data were collected from the most recent examinations before surgery.

Collection of liver tissue homogenate and enzyme-linked immunosorbent assay

To collect tissue homogenate, surgically excised liver tissues were freshly harvested and cut into small pieces after PBS (0.01 M, pH 7.4) flushing. The 0.1 g liver tissues were transferred into a glass homogenizer with 0.9 mL of pre-cooled PBS. After the liver tissues were thoroughly ground to homogenization, the supernatant was collected and filtered through a 0.22- μm filter to remove any impurities before detection.

Following the manufacturers’ instructions (Adsbio, Jiangsu, China), ELISA kits were used to detect the concentrations of growth differentiation factor 15 (GDF15; 2305H16), fibroblast growth factor 21 (FGF21; 2305H22), interleukin-1 β (IL-1 β ; 2305H19), tumor necrosis factor- α (TNF- α ; 2305H12), interleukin-10 (IL-10; 2305H25), transforming growth factor β (TGF- β ; 2305H33), and chemokine C-C motif ligand 2 (CCL2; 2305H36) in liver tissue homogenate.

Histopathology

Surgically excised liver tissues were kept in 4% paraformaldehyde. Fixed liver tissues were embedded in paraffin, cut into 3 μm sections, and stained with H&E. The samples were finally imaged and scored under light microscopy. The histopathological scores were assessed based on the “Guideline for diagnosis and treatment of liver failure (2018).” The ACLF pathological score was given according to the extent of liver tissue necrosis. Normal liver tissue structure received a score of 0; spotty necrosis, fusion necrosis, and bridging necrosis received a score of 2; massive hepatic necrosis affecting approximately 1/2–2/3 of hepatic parenchyma received a score of 3; and massive hepatic necrosis affecting more than 2/3 of the hepatic parenchyma received a score of 4.

Immunohistochemical staining

Immunohistochemical staining of liver sections was performed. Several 3- μm sections were prepared from paraffin-embedded blocks of tissue. Sections were dewaxed, rehydrated by fractionated alcohol series, and heated in a microwave oven for 5 min in 10 mm sodium citrate (pH 6.0) to recover antigens. After antigen retrieval, paraffin sections were placed in 3% H₂O₂ and blocked for 10 min to eliminate endogenous peroxidase activity. Then, the samples were blocked and incubated with 10% goat serum for 30 min. The rabbit anti-human HIF-1 α (1:200, Bioss, Beijing, China) was added as the primary antibody and incubation was done overnight at 4 °C, in a humidified box. Then, the secondary antibody was added dropwise before incubation at 37°C for 30 min. DAB was added as the substrate to enhance color development. When the color change was observed, the staining solution was immediately washed off with tap water. Hematoxylin

was counterstained for 3 min, differentiated with 1% hydrochloric acid and alcohol, and rinsed with tap water for 10 min. Gradient alcohol dehydration was performed. Xylene was transparent, and the film was mounted with a neutral gum. The number of HIF-1 α positive cells was quantified, and images were captured under a microscope. The Image J software (NIH Image, Bethesda, MD, United States) was used for analysis.

Immunofluorescence staining

For double immunofluorescence staining, paraffin-embedded tissues were cut into 3.5 mm sections. Each section was deparaffinized and blocked with EDTA (pH 8.0) antigen repair solution (1:49, Aifang, Changsha, China) at 96°C for 20 min. Then, the sections were incubated overnight at 4°C with the following primary antibodies: Mouse anti-human CD68 (1:200, Aifang, Changsha, China), mouse anti-human Ki67 (1:200, Boster, Wuhan, China), rabbit anti-human HLA-DR (1:300, Abcam, Cambridge, United Kingdom), rabbit anti-human CD206 (1:200, Aifang, Changsha, China), and mouse anti-human CD163 (1:150, Aifang, Changsha, China). The samples were then incubated with FITC tag goat-anti-rabbit IgG (1:500), FITC tag goat-anti-mouse IgG (1:500), cy3 tag goat-anti-rabbit IgG (1:500), and cy3 tag goat-anti-mouse IgG (1:500) for 1 h. The sections were slightly dried and incubated with the DAPI staining solution (Solarbio, Beijing, China) at room temperature and in the dark, for 10 min. After DAPI staining for 5 min, the sections were washed with PBS three times. Each of the three washing procedures was done for 5 min. The washed sections were then sealed with an anti-fluorescence attenuated sealing solution that contained DAPI. Fluorescence images were scanned using a digital pathology scanner (KF-FL-020, Zhejiang, China) and images were captured. The results were analyzed using the Image J software (NIH Image, Bethesda, MD, United States).

TEM

The liver tissue was dissected into 1-mm pieces and fixed in 4% paraformaldehyde and 0.1 M sodium cacodylate buffer (pH 7.2) containing 2% glutaraldehyde, at 4°C overnight. After three times of washing in buffer, the samples were post-fixed in 2% osmium tetroxide and 1% uranyl acetate for 2 h, rinsed in water, dehydrated in ascending ethanol series and 100% acetone, before it was infiltrated and embedded in eponate. Ultrathin sections were cut using a Leica EM UC7. The sections were exposed to the primary stain (5% aqueous uranyl acetate). They were then exposed to the secondary stain (lead citrate) and visualized using a 120 kv TEM HT7800 (Hitachi, Japan). Five random fields of view were imaged per group to quantify the size and number of mitochondria. Mitochondria were identified based on their morphology. Mitochondrial length, width, and cross-sectional area were measured using Image Pro-Plus 6.0 software (Media Cybernetics, Silver Spring, MD, United States). Mitochondrial count analysis was performed at the original magnification of 7000.

Targeted metabolomics

Ultra-high performance liquid chromatography-tandem mass spectrometry (UPLC-MS/MS) system (Waters XEVO TQ-S Micro, Waters Corporation) was used for targeted metabolomics analysis of 16 organic acids in liver samples. Briefly, 17 liver samples from patients with HBV-ACLF and 12 liver samples from HDs were collected and stored in an Eppendorf Safelock microcentrifuge tube. The centrifuge tube was placed in a low-temperature centrifuge and centrifuged at 12000 rpm at 4 °C for 5 min. Then, 50 μ L of supernatant were taken and 50 μ L of propionic acid isotope internal standard (IS; 5 μ g/mL) and 50 μ L of 3-nitrophenylhydrazine (250 mmol/L, prepared with 50% methanol/aqueous solution) were added to it. Thereafter, 50 μ L of 1-Ethyl-3-(3-dimethylaminopropyl) carbodiimide (150 mmol/L, prepared with 75% methanol/aqueous solution (containing 7.5% pyridine)) was added and placed in a shock mixer at 30°C for 30 min. The supernatant was extracted by adding 50 μ L of 2, 6-di-tert-butyl-p-cresol methanol solution (2 mg/mL) and 250 μ L of 75% methanol solution at 12000 rpm for 5 min, and then used for LC-MS analysis.

Chromatographic separation was performed using Waters ACQUITY UPLC I-CLASS ultra-high performance liquid chromatography with a Waters UPLC BEH C18 column (2.1 mm \times 100 mm I.D., 1.7 μ m; Waters Corp., Milford, MA, United States) at a column temperature of 40°C. The mobile phase was composed of 0.1% formic acid aqueous solution (A). The methanol: Isopropyl alcohol ratio was 8:2 (B). The flow rate was 0.30 mL/min, and the injection volume was 5 μ L.

Multireaction monitoring of 16 organic acids (IS) was performed using the Waters XEVO TQ-S Micro series four-bar mass spectrometry system. The optimal Mass Spectrometric parameters were as follows: Ion source voltage was 3.0 kV, temperature was 150°C; desolvation temperature was 450°C, desolvation gas flow rate was 1000 L/h; cone-hole gas flow rate was 10 L/h.

Data acquisition and processing were conducted using the MassLynx 4.1 software (Waters Corp., Milford, MA, United States), and the concentration of each metabolite was calculated based on the standard curve. The calculated concentrations of organic acids were imported into the SIMCA software (v. 14.1, Umetrics, Sweden) for multivariate analyses, including orthogonal partial least squares-discriminant analysis (OPLS-DA) and replacement test. Finally, differential metabolites were used for pathway enrichment analysis.

Statistical analysis

Statistical analyses were performed using the SPSS software (ver. 21.0; IBM Corp., Armonk, NY, United States), and the figures were produced using Prism 8.0 (GraphPad Software, San Diego, CA, United States). All values are presented as mean \pm SE of mean, median (interquartile range), or numbers (%). For single comparisons, the unpaired Student's *t*-test was used for data with normal distribution, and the Mann-Whitney test was used for data with non-normal distribution. Categorical variables were compared using chi-squared tests. The Pearson test was used for determining the correlations for normally distributed variables. The Spearman test was applied to measure the correlations of non-normal variables. A

P value of less than 0.05 indicated statistical significance.

RESULTS

Baseline characteristics

Table 1 summarizes the baseline characteristics, demographic, and laboratory features of patients. The two groups were comparable with regard age and sex, and all patients in the ACLF group were male. All patients with ACLF had liver cirrhosis, and five cases in the HD group had metabolic associated fatty liver disease. Compared with the HD group, the ACLF group had lower levels of WBC, PLT, ALB, sodium, and PT, but higher levels of TBIL, AST, ALT, and INR. Moreover, the PTA of the ACLF group was lower than the lower limit of normal, and the hs-CRP, PCT, LAC, and NH₃ were more than the upper limit of normal. The mean MELD score of patients in the ACLF group was 28.65, with each individual having a MELD score of greater or equal to 19, suggesting a high risk of end-stage liver disease. In the ACLF group, the mean MELD-Na score was 32.83, and the mean COSSH-ACLF II score was 7.69. More than 65% of patients with ACLF were exposed to an intermediate to high risk of end-stage liver disease (**Table 1**).

Liver histopathology

Under the light microscope, the following observations were made: the structure of the liver tissue of some HDs was complete and clear; the structure of liver lobules was clear and normal; the volume of hepatocytes was uniform; the nuclei were in the middle; and the cytoplasm was red-stained. The hepatocytes were arranged radially around the central vein, and there was no sign of necrosis, steatosis, fibroplasia, and inflammatory infiltration. The liver of the others showed diffuse fatty lesions, disordered lobular structure, deranged hepatic cords, ballooned or swollen hepatocytes, loose cytoplasm, diffuse lipid droplets of different sizes in the cytoplasm, and a small number of punctate necrosis. Pathologic assessment of the liver in patients with ACLF showed destruction of the normal structure as well as collapse or incomplete collapse of reticular scaffolds. The liver tissue showed massive or submassive necrosis, along with abundant inflammatory cell infiltration. The percentage of normal hepatocytes significantly decreased. Hepatic sinusoids were significantly dilated, congested, and even hemorrhagic. Circular or triangular portal areas were observed around necrosis. Massive bile ducts, in the form of tubes or branches, were observed around the edge of the necrotic zone and the confluence area. Cholestasis and bile plugs were seen in some of the lumens. The hepatic lobules were structurally disorganized, with massive extracellular matrix hyperplasia. Residual hepatocytes were wrapped and segmented into nodules of varying sizes by fibrous septae. Hepatocytes in the residual nodules showed various degrees of hepatocyte ballooning. Some hepatocytes were eosinophilic, and apoptotic bodies and binucleated hepatocytes were visible (**Figure 1A**). Histopathological scoring showed that hepatocyte necrosis markedly increased in the liver of patients with ACLF compared with the HDs, and the difference was statistically significant (**Figure 1B**).

Upregulated hypoxia markers in patients with ACLF

The transcription factor HIF-1 α mediates the adaptive response to hypoxia. In normoxic conditions, HIF-1 α is hydroxylated and rapidly degraded. Hypoxia upregulates HIF-1 α and promotes its translocation to the nucleus to form a complex with HIF-1 β . This promotes the transcription of genes that are essential for hypoxic adaptation[6]. The expression of key mediators of hypoxia in the liver samples was examined through immunohistochemistry to assess whether patients with ACLF suffered from anoxia whammy. The results from immunohistochemical staining demonstrated that the expression of HIF-1 α was elevated in the cytoplasm and nucleus of hepatocytes in patients with ACLF compared with the HDs. This showed significant hypoxic injury in patients with ACLF (**Figure 2**).

Altered mitochondrial ultrastructure in the liver of patients with ACLF

TEM images with different magnifications are shown in **Figure 3A**. In HDs, mitochondrial morphology, cristae, and matrix were intact and orderly arranged. Compared to normal mitochondrial conformation in HDs, mitochondrial ultrastructure was severely disorganized in the liver of patients with ACLF. Some mitochondria were severely swollen and transformed into vacuolated structures with abnormal mitochondrial morphology. The mitochondrial outer membrane was mostly incomplete, while the cristae were sparse, disorganized, or absent. The density of the mitochondrial matrix was lower and filled with an electron-dense material in patients with ACLF, suggesting extensive mitochondrial degeneration. A small number of autophagosomes and autophagic lysosomes were seen in the liver of patients with ACLF (**Figure 3A**). Compared with HDs, the liver of patients had an increased number of mitochondria in each microscopic field. The length, width, and area of the mitochondria also increased (**Figure 3B** and **C**), as part of the repair response after liver injury.

Mitochondrial dysfunction in patients with ACLF

TEM showed severe ultrastructural damage of mitochondria in the livers of patients with ACLF. GDF15 and FGF21 Levels in tissue homogenates were examined to reveal mitochondrial dysfunction. GDF15 and FGF21 are circulating markers for mitochondrial disorders and are widely used in diagnosis of mitochondrial diseases[7-9] and other serious diseases, such as liver failure[4,10,11], heart failure[12,13], and sepsis[14,15]. Their expression levels positively correlated with disease severity. The expression of GDF15 in liver homogenates of patients with ACLF increased compared to the HD group (**Figure 3D**). This revealed mitochondrial dysfunction in patients with ACLF. Nevertheless, FGF21 Levels were significantly lower in patients with ACLF compared to the HDs (**Figure 3E**). In contrast, plasma FGF21 levels were higher

Table 1 Baseline characteristics of the included patients

Variable	HD (n = 16)	ACLF (n = 17)	P value
Age (yr)	47.24 ± 2.01	52.18 ± 4.16	0.2964
Gender [male, n (%)]	14 (87.5)	17 (100)	0.227
Other liver disorders, n (%)			
Cirrhosis	0 (0)	17 (100)	< 0.0001
MAFLD	5 (31.25)	0 (0)	0.044
None	11 (68.75)	0 (0)	< 0.0001
Laboratory measurements			
WBC (× 10 ⁹)	14.01 (7.69)	7.86 ± 1.07	< 0.0001
NEUT (%)	78.20 (19.50)	71.90 (14.95)	0.1705
PLT (× 10 ⁹)	199.44 ± 26.26	70.00 ± 8.80	0.0002
TBIL (μmol/L)	10.16 ± 1.01	332.05 ± 51.60	< 0.0001
AST (IU/L)	36.00 (35.55)	94.50 (83.15)	0.0106
ALT (IU/L)	24.00 (41.05)	67.50 (67.8)	0.0281
ALB (g/L)	42.98 ± 0.86	37.25 ± 1.26	0.0007
Sodium (mmol/L)	142.32 ± 1.43	135.40 ± 1.48	0.0023
CREA (μmol/L)	71.00 (28.40)	64.00 (39.50)	0.8717
BUN (mmol/L)	5.69 (3.24)	5.40 (6.30)	0.8094
PT (S)	12.29 ± 0.36	27.36 ± 2.28	< 0.0001
INR	1.02 ± 0.04	2.56 ± 0.26	< 0.0001
PTA (%)	ND	28.00 (31.00)	ND
hs-CRP (mg/L)	ND	8.41 (8.73)	ND
PCT (ng/mL)	ND	0.51 (0.37)	ND
LAC (mmol/L)	ND	2.78 ± 0.21	ND
NH ₃ (μmol/L)	ND	84.9 ± 10.19	ND
ESR (mm/h)	ND	10.00 (9.5)	ND
ACLF risk scores			
MELD score	ND	28.65 ± 1.42	ND
MELD category, n (%)			
1: ≥ 40	ND	1 (5.9)	ND
2: 30-39	ND	8 (47.1)	ND
3: 20-29	ND	7 (41.1)	ND
4: 15-19	ND	1 (5.9)	ND
MELD-Na (score)	ND	32.83 ± 2.42	ND
COSSH-ACLF II score	ND	7.69 ± 0.30	ND

All values are expressed as mean ± SEM, median (IQR), or number (percentages). Data with normal distribution were compared using unpaired student's *t*-test, and the Mann-Whitney test was used for data without non-normal. Categorical variables were compared using chi-squared tests.

MAFLD: Metabolic associated fatty liver disease; NEUT: Neutrophilic granulocyte; PLT: Platelet; TBIL: Total bilirubin; AST: Aspartate transaminase; ALT: Alanine transaminase; ALB: Albumin; CREA: Creatinine; BUN: Blood urea nitrogen; PT: Prothrombin time; INR: International normalized ratio; PTA: Prothrombin time activity; hs-CRP: Hypersensitive C-reactive protein; PCT: Procalcitonin; LAC: Lactate; ESR: Erythrocyte sedimentation rate; MELD: Model for end-stage liver disease; MELD-Na: Model for end-stage liver disease includes serum sodium; COSSH-ACLF II: Chinese group on the study of severe hepatitis B- acute-on-chronic liver failure II; HD: Healthy donor; ACLF: Acute-on-chronic liver failure; ND: Not determined.

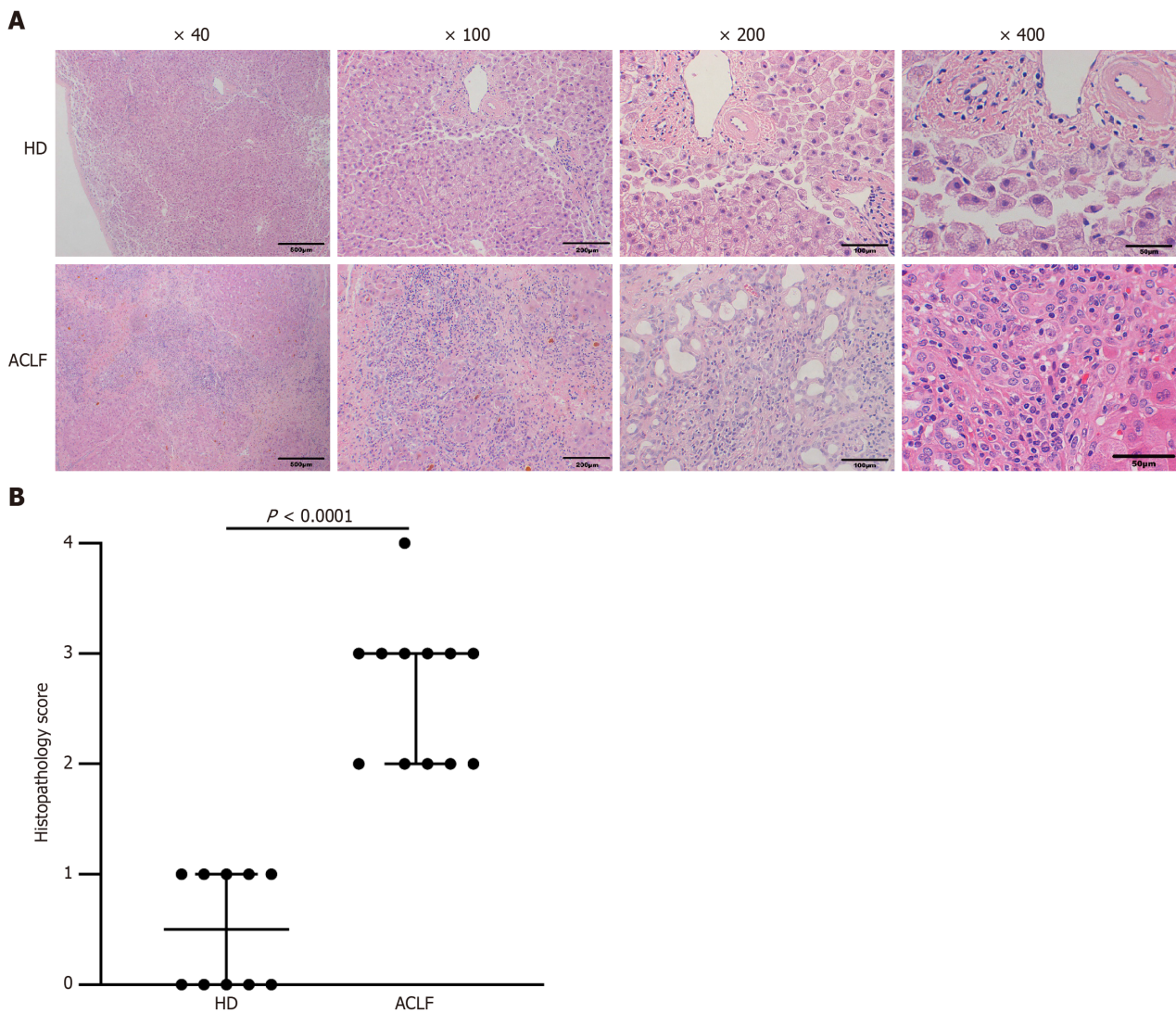


Figure 1 Liver histopathology in healthy donors and patients with acute-on-chronic liver failure. A: HE staining of the liver tissue from healthy donors ($n = 10$) and patients with acute-on-chronic liver failure ($n = 12$); B: Histopathological Scoring. Data were compared using Mann-Whitney test. ACLF: Acute-on-chronic liver failure; HD: Healthy donor.

in patients with ACLF in some studies[6,11]. Some studies reported that plasma levels of FGF21 were not associated with the severity of ACLF[11].

Metabolic profiles of liver in patients with ACLF

Mitochondria drive metabolic adaption to environments. This study investigated whether mitochondrial dysfunction in patients with ACLF was accompanied by metabolic change. Therefore, the levels of organic acid metabolites in tissues of HDs and ACLF patients were determined through targeted metabolomics. A total of 16 different types of organic acids were quantified. The concentrations of the 16 organic acids were imported into the SIMCA software for OPLS-DA. The results are shown in the OPLS-DA scatter diagram (Figure 4A). The OPLS-DA model effectively differentiated between HD and ACLF samples, suggesting that there were differences in total organic acid metabolites between HDs and patients with ACLF, with lower inter-sample variability among patients with ACLF. The 200 permutation tests of our data demonstrated no overfitting in the OPLS-DA model [$Q^2 = (0.0, -0.474)$; Figure 4B]. The hierarchical cluster analysis showed that the 16 organic acids could differentiate between ACLF patients and HDs (Figure 4C). Volcano plots were used to identify fumarate, methylmalonic acid, succinate, α -ketoglutaric acid, LAC, phenylacetic acid, and ethylmalonic acid as differential metabolites (Figure 4D).

Statistical analysis of data from targeted metabolomics revealed seven differential organic acids. Compared with HDs, fumarate and methylmalonic acid levels decreased in patients with ACLF, whereas succinate, α -ketoglutaric acid, LAC, phenylacetic acid, and ethylmalonic acid levels increased in these patients (Figure 4E). The LAC /pyruvate ratio, a surrogate marker for the cytosolic NADH/NAD⁺ ratio and a hallmark of the redox state[16] was also calculated. The LAC /pyruvate ratio was significantly elevated in patients with ACLF compared to HDs (Figure 4E), suggesting enhanced anaerobic glycolysis. The liver in patients with ACLF patients used the extra-mitochondrial pathways to generate ATP. The seven differential organic acids were imported into the MetaboAnalyst website (<https://www.metaboanalyst.ca/>) for metabolic pathway enrichment analysis. The pathway enrichment analysis identified six pathways ($P < 0.05$) enriched

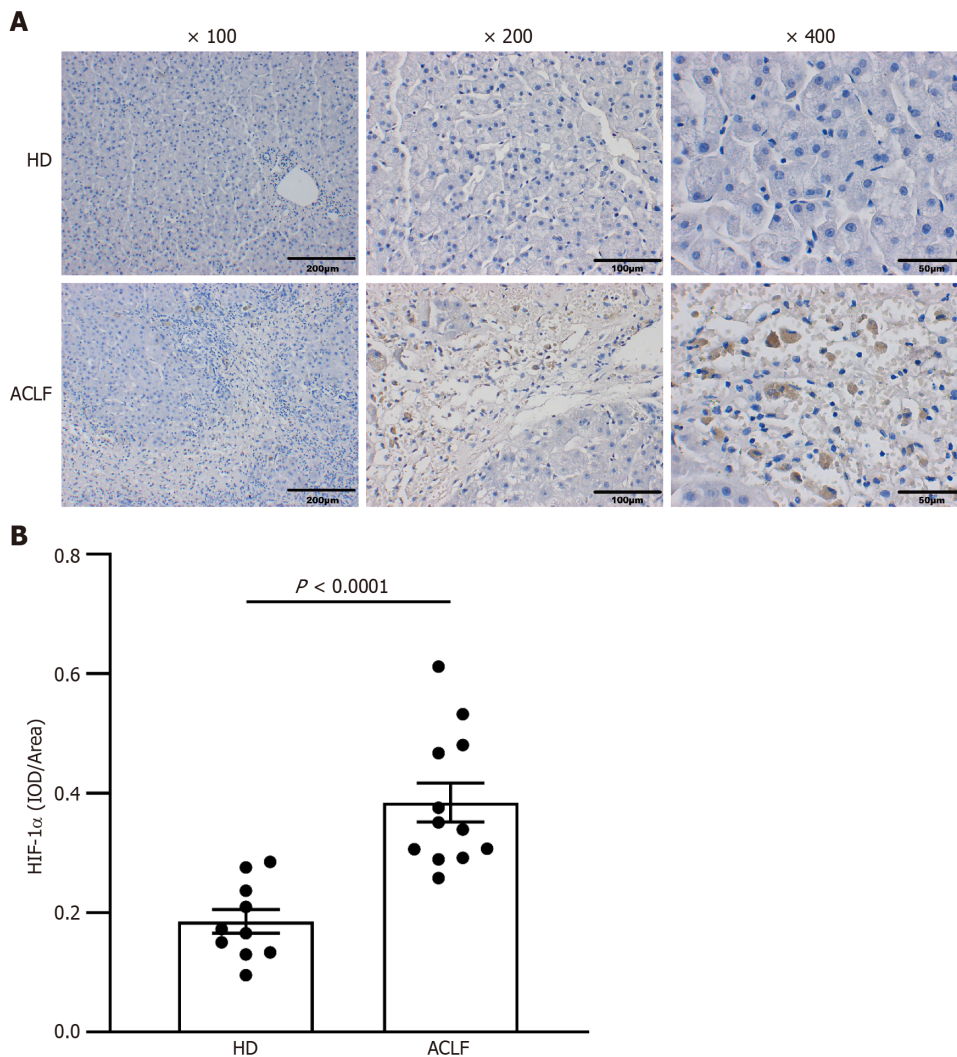


Figure 2 Expression of hypoxia-inducible factor-1α increased in the liver tissues of patients with acute-on-chronic liver failure. A: Immunohistochemical staining of hypoxia-inducible factor-1α (HIF-1α); B: Semi-quantitative analysis of HIF-1α expression. Data were compared using unpaired student's *t*-test. ACLF: Acute-on-chronic liver failure; HD: Healthy donor; HIF-1α: Hypoxia-inducible factor-1α.

in ACLF (Figure 4F). These pathways play key roles in glucose metabolism, fatty acid metabolism, and amino acid metabolism.

Widespread macrophages activation in the liver of patients with ACLF

Mitochondrial dysfunction affected liver metabolism in patients with ACLF. Double immunofluorescence staining with anti-ki67 and anti-CD68 antibodies was used to label proliferating macrophages and determine whether metabolic transformation affected hepatic macrophages (Figure 5A). There was no statistically significant difference in cell proliferation (Ki67⁺) between HDs and patients with ACLF (Figure 5B). However, there was significant macrophage (CD68⁺) infiltration in the liver of ACLF patients (Figure 5C). Double immunofluorescence staining with Ki67 and CD68 showed no significant differences in the number of proliferating macrophages between the groups (Figure 5D), suggesting that the infiltrating macrophages originated from peripheral circulating monocytes rather than liver-resident macrophages (*i.e.*, Kupffer cells). CCL2, a key chemokine that regulates monocyte/macrophage migration and infiltration, was overexpressed in the liver of patients with ACLF (Figure 5E), suggesting an increased capacity of circulating monocytes for hepatic infiltration in patients with ACLF.

Impaired macrophage polarization in the liver of patients with ACLF

Macrophages can acquire different phenotypes depending on environmental and immune signals. They are mainly classified into two major groups: (1) Classically activated macrophages endowed with pro-inflammatory and microbicidal functions and (2) alternatively activated macrophages with anti-inflammatory and tissue remodeling properties. The classically activated macrophages (CD68⁺ HLA-DR⁺) and alternatively activated macrophages (CD163⁺ CD206⁺) were labeled *via* double immunofluorescence staining (Figure 6A and B) to determine whether there was a phenotypic change in hepatic macrophages. The results showed that the abundance of CD68⁺ HLA-DR⁺ macrophages increased (Figure 6C), while the abundance of CD163⁺ CD206⁺ macrophages decreased in patients with ACLF compared to HDs (Figure 6D). Macrophages were polarized toward the classically activated phenotype (Figure 6E). The results from

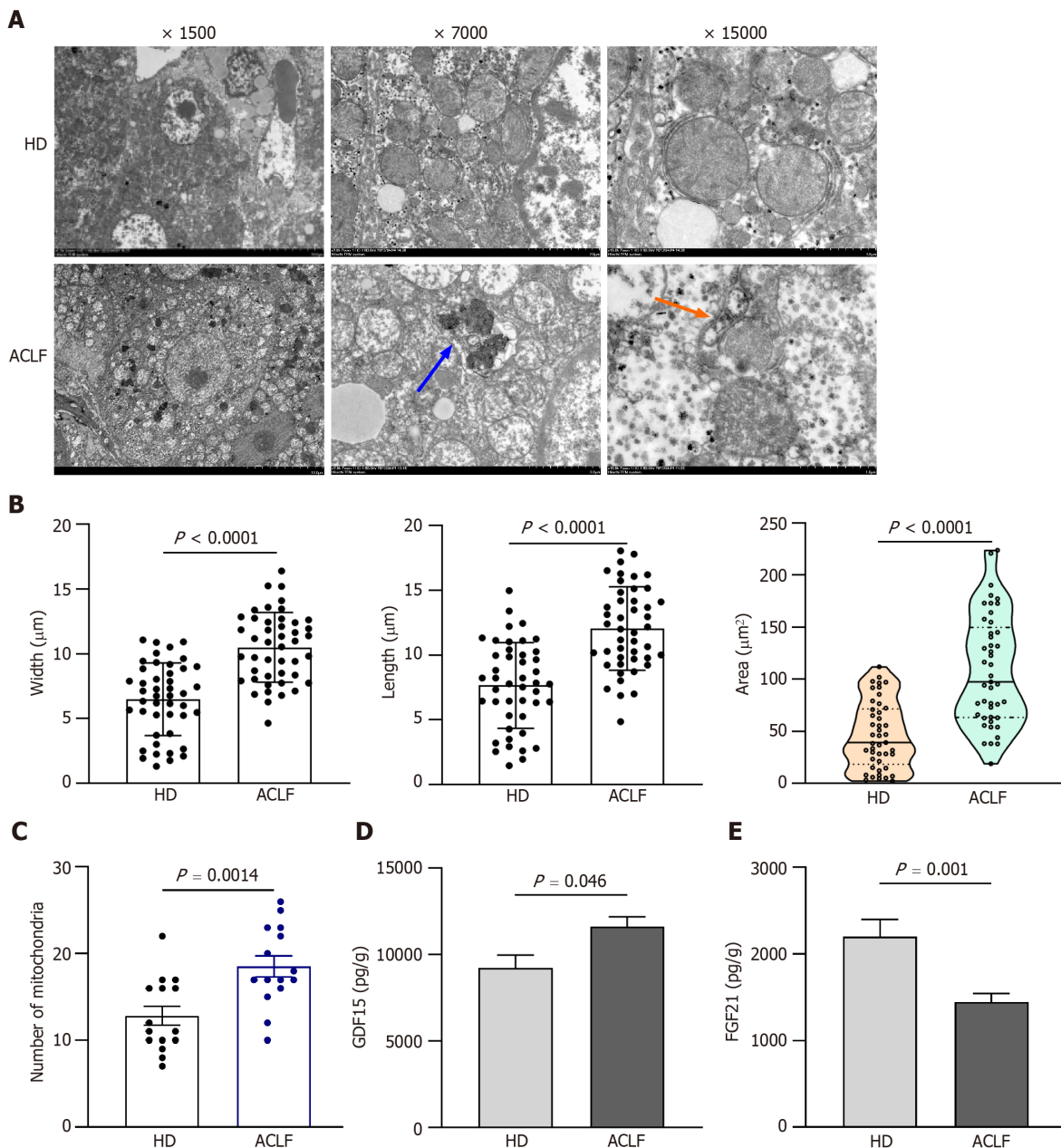
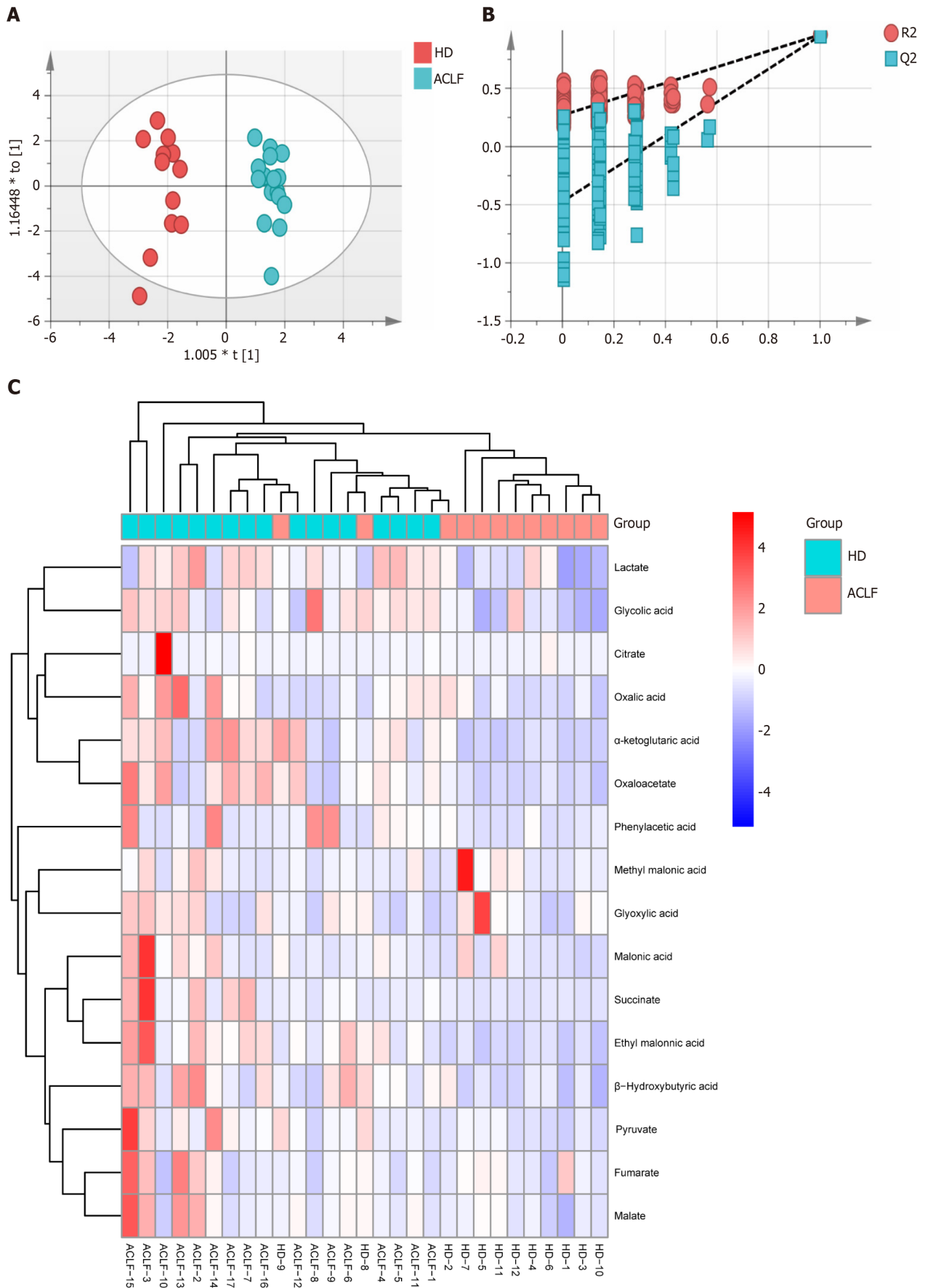


Figure 3 Mitochondrial morphology and function in the liver of patients with acute-on-chronic liver failure. A: Representative electron microscopy images of hepatic mitochondria from 3 patients with acute-on-chronic liver failure (ACLF) and 3 healthy donors (HDs). Orange arrows indicate autophagosome; the blue arrow indicates autophagic lysosome; B: Length, width, and area of each mitochondrion; C: Number of mitochondria at original magnification of 7000; D: Growth differentiation factor 15 levels in liver homogenates of 12 HDs and 17 patients with ACLF; E: Fibroblast growth factor 21 levels in liver homogenates. Data with normal distribution were compared using unpaired student's *t*-test, and the Mann-Whitney test was used for non-normal data. ACLF: Acute-on-chronic liver failure; HD: Healthy donor; GDF15: Growth differentiation factor 15; FGF21: Fibroblast growth factor 21.

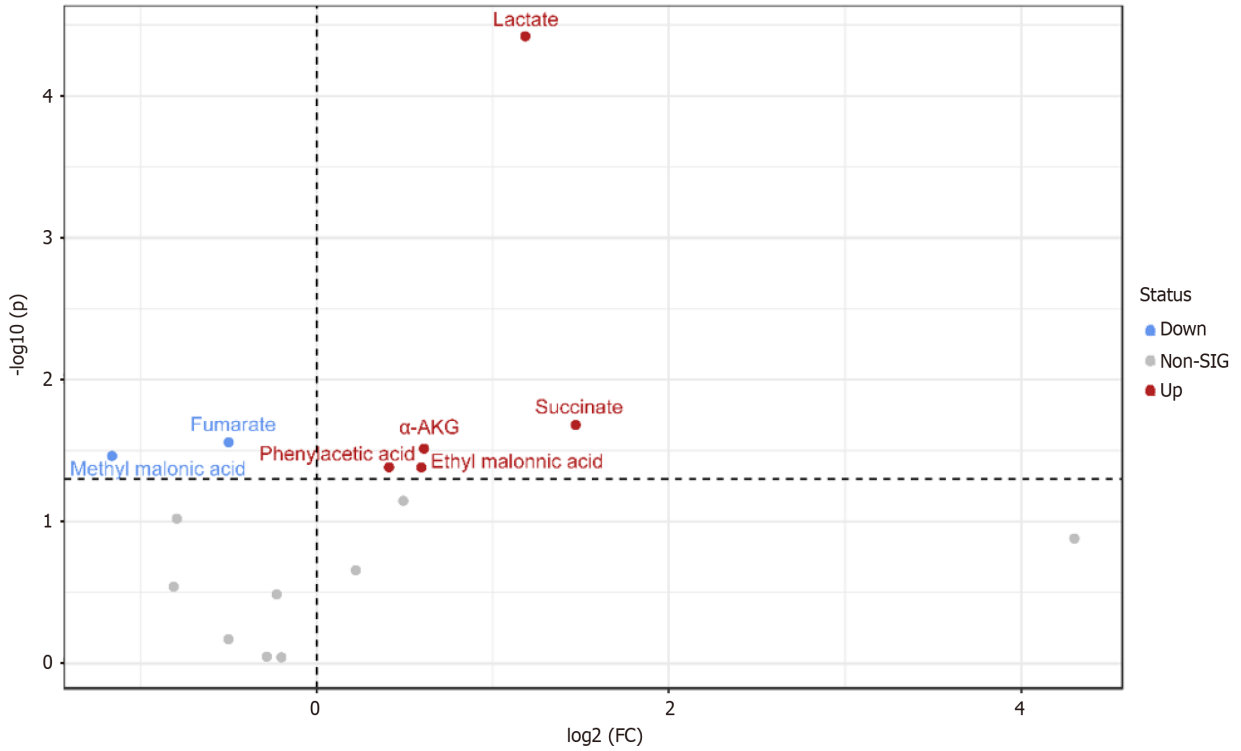
the cytokine assay were consistent with those from immunofluorescence. Compared with HDs, patients with ACLF exhibited elevated expression of IL-1 β and TGF- β 1 (Figure 6F). IL-1 β is a CD68⁺ HLA-DR⁺ macrophage-derived pro-inflammatory cytokine and TGF- β 1 is a potent pro-fibrotic factor. As a CD163⁺ CD206⁺ macrophage-derived anti-inflammatory cytokine, IL-10 was downregulated in patients with ACLF (Figure 6F). There was no significant difference in TNF- α levels between the groups (Figure 6F).

The relationship between metabolic remodeling and macrophage activation

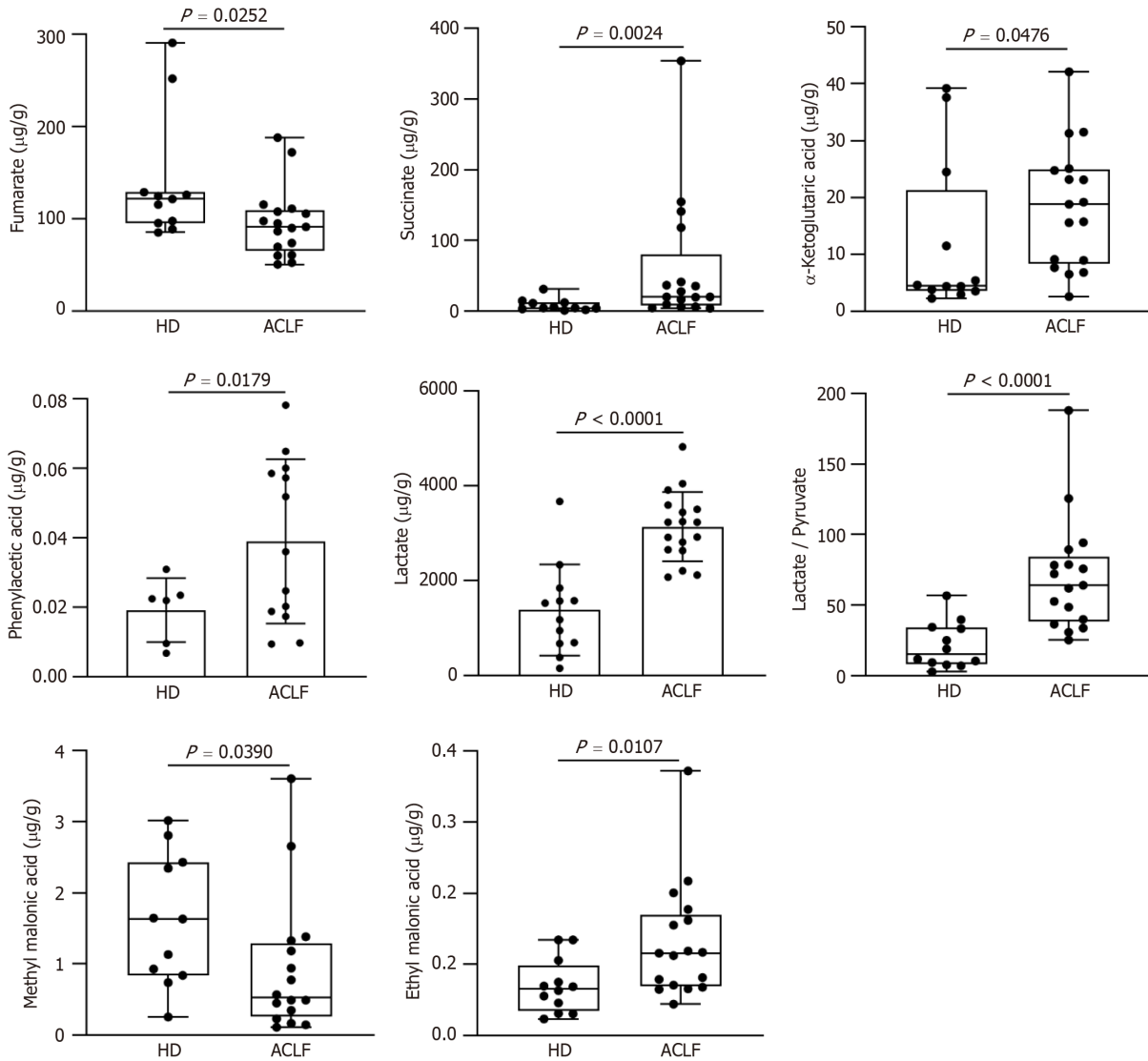
Macrophages undergo extensive metabolic rewiring upon activation, increasing the abundance of specific metabolites [17]. They act as co-factors for enzymes and posttranslationally modify histones. They also affect the function of transcription factors, enzymes, and other key proteins, thereby regulating cellular phenotypes [18]. The correlation between 16 organic acid metabolites and macrophage-derived cytokines/chemokines was analyzed to investigate whether the metabolic changes affected the immune inflammatory response in patients with ACLF (Figure 7A). The results showed that IL-1 β levels positively correlated with those of pyruvate, fumarate, malate, ethyl malonic acid, glyoxylic acid, and β -Hydroxybutyric acid, while negatively correlating with those of citrate ($P < 0.05$). The correlation



D



E



F

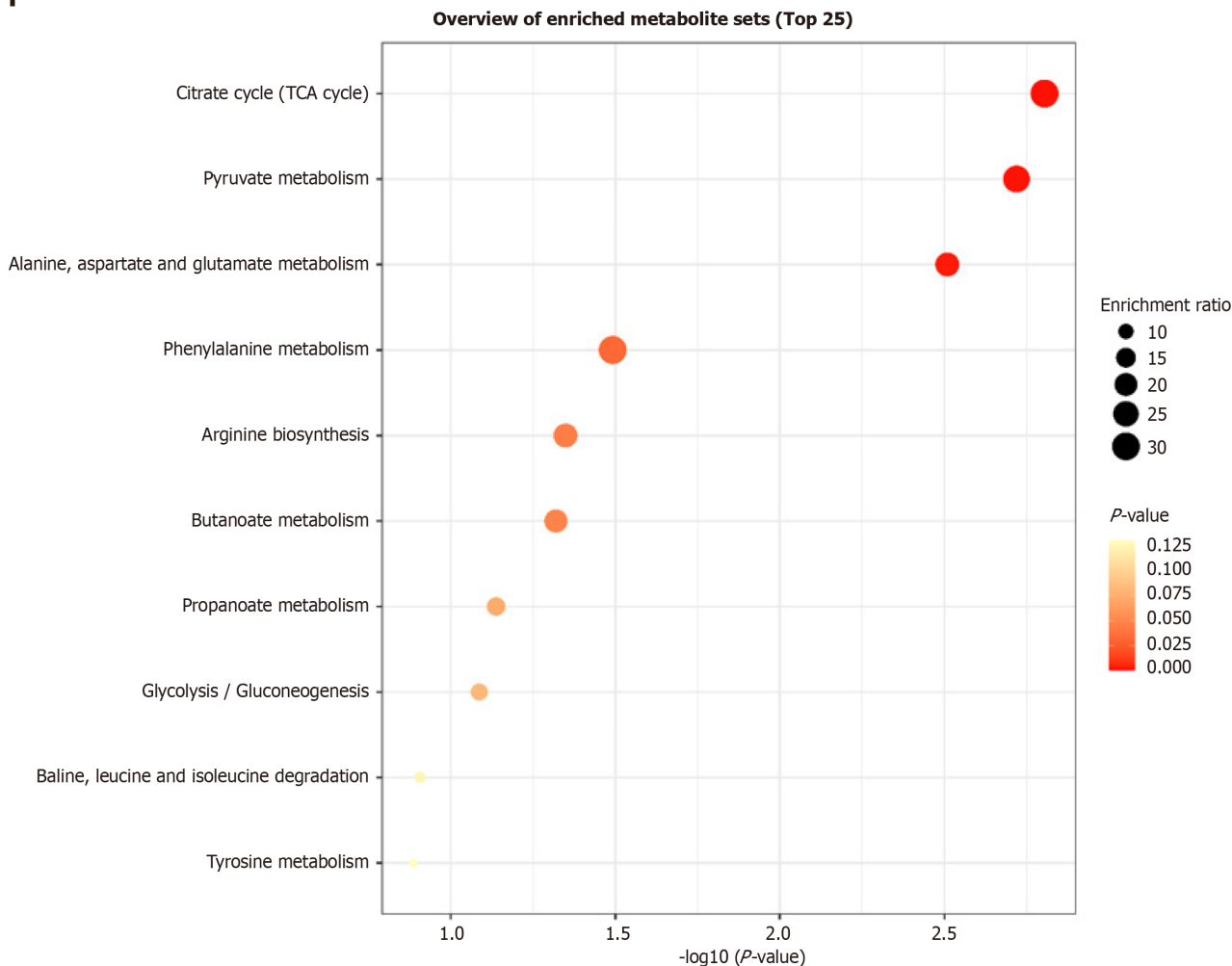


Figure 4 Metabolic profiles of the liver of patients with acute-on-chronic liver failure. A: Orthogonal partial least squares-discriminant analysis scatter plot; B: Permutation tests; C: Hierarchical clustergram of organic acid metabolites; D: Volcano plot comparing organic acid metabolites between patients with acute-on-chronic liver failure ($n = 17$) and healthy donors ($n = 12$); E: Quantitative analysis of differentially expressed organic acid metabolites; F: Kyoto Encyclopedia of Genes and Genomes pathway enrichment analysis. Data with normal distribution were compared using unpaired student's *t*-test, and the Mann-Whitney test was used for non-normal data. ACLF: Acute-on-chronic liver failure; HD: Healthy donor.

coefficients were 0.671, 0.671, 0.738, 0.603, 0.736, 0.559, and -0.644, respectively (Figure 7B). TNF- α levels positively correlated with those of LAC ($P < 0.05$), with a correlation coefficient of 0.665 (Figure 7B). IL-10 levels negatively correlated with those of pyruvate, fumarate, malate, and methyl malonic acid ($P < 0.05$), and the correlation coefficients were -0.635, -0.612, -0.535, and -0.621, respectively (Figure 7B). TGF- β 1 Levels positively correlated with those of fumarate, malate, methyl malonic acid, ethyl malonic acid, and glyoxylic acid, while negatively correlating with citrate ($P < 0.05$). The correlation coefficients were 0.568, 0.618, 0.589, 0.544, 0.557, and -0.518, respectively (Figure 7B). CCL2 levels positively correlated with those of glycolic acid ($P < 0.05$), with a correlation coefficient of 0.665 (Figure 7B). Organic acid metabolites strongly and positively correlated with pro-inflammatory cytokines and negatively correlated with anti-inflammatory cytokines. IL-1 β was strongly associated with tricarboxylic acid (TCA) cycle intermediates. Succinate is a novel driver of inflammation, which can be sensed by succinate receptor 1[19,20]. The intracellular succinate in macrophages stabilizes HIF-1 α , thereby enhancing IL-1 β production in normoxic conditions[21]. Lactate not only provides energy for cell growth but also acts as an important signaling molecule for regulating the function of immune cells[22]. In hypoxic conditions, macrophages exhibit enhanced migratory capacity partly through HIF-1 α signaling to redirect pyruvate from the TCA cycle to LAC production, thereby enhancing localized energy generation[23].

DISCUSSION

Viral, immune, and metabolic processes are involved in the development and progression of HBV-ACLF. The metabolic characteristics of patients with HBV-ACLF profoundly change, mainly due to hyperammonemia and hypoxia[3]. Severe systemic inflammation in ACLF is associated with the accumulation of metabolites in the body, along with profound metabolic alterations, such as mitochondrial dysfunction[24]. Mitochondrial dysfunction governs immunometabolism in

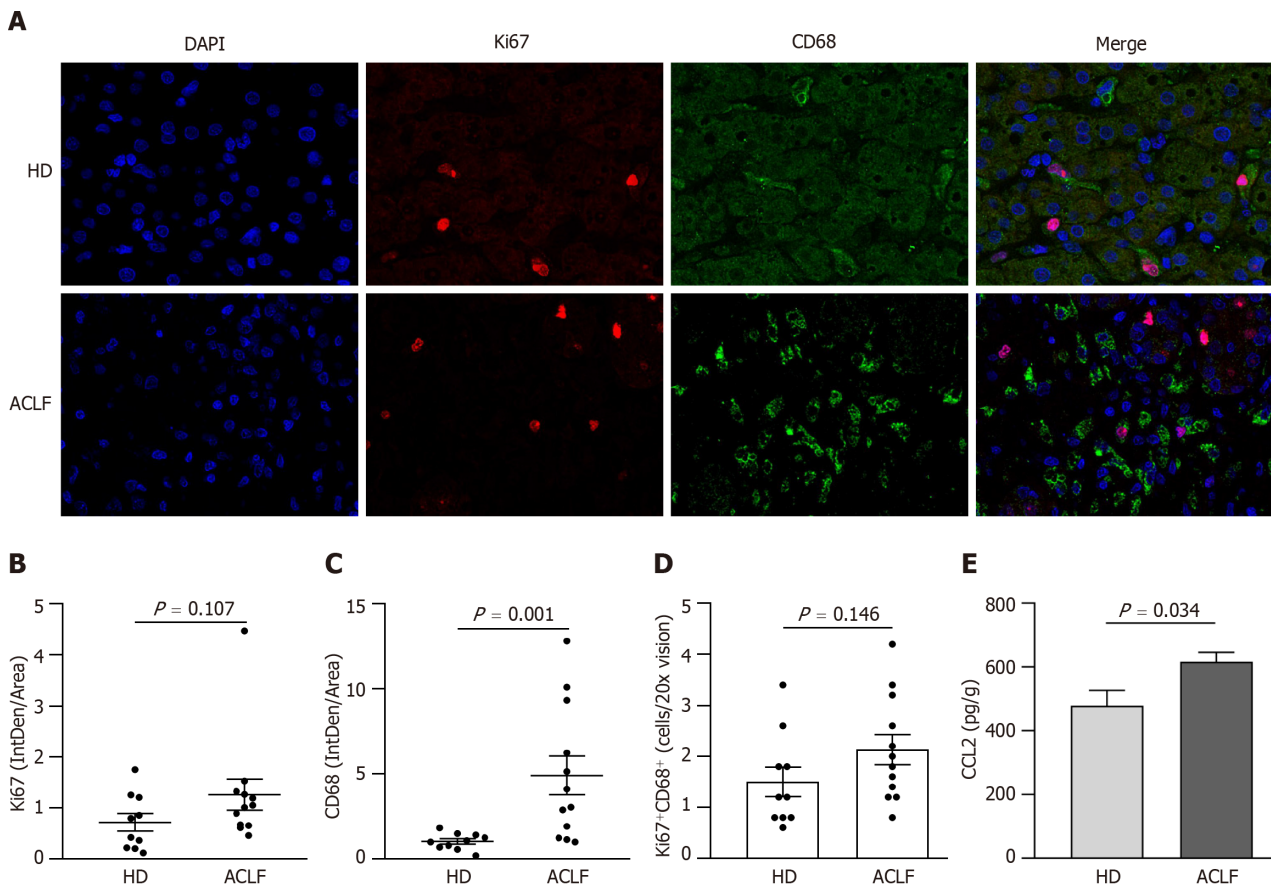


Figure 5 Macrophages were widely activated in the liver of patients with acute-on-chronic liver failure. A: Representative microscopic images of the double immunofluorescence staining of Ki67 and CD68 in the liver (400 fold). The red fluorescence signal represented Ki67; the green fluorescence signal represented CD68; and the blue fluorescence signal represented DAPI; B: Ki67 immunofluorescence intensity in the liver of healthy donors ($n = 10$) and patients with acute-on-chronic liver failure ($n = 12$); C: CD68 immunofluorescence intensity in the liver; D: The mean number of Ki67⁺ CD68⁺-positive cells in five \times 200 fields; E: Chemokine C-C motif ligand 2 levels in liver homogenates. Data with normal distribution were compared using unpaired student's *t*-test, and the Mann-Whitney test was used for non-normal data. ACLF: Acute-on-chronic liver failure; HD: Healthy donor.

the leukocytes of patients with ACLF[4]. This study is the first to describe changes in the bioenergetics of the liver in patients with advanced HBV-ACLF. Bioenergetic alteration driven by hypoxia and mitochondrial dysfunction contribute to hepatic immune and metabolic remodeling, which may cause organ failure and poor clinical prognosis in patients with advanced HBV-ACLF. In this study, the data were obtained from the liver of patients with HBV-ACLF, whose mitochondrial function, metabolites, and immune microenvironment were less susceptible to any confounding factors caused by other failing organs.

Massive inflammatory cell infiltration was observed in the liver tissue of HBV-ACLF patients in histopathological assessment. CCL2 levels were elevated in the liver tissue of HBV-ACLF, indicating increased chemotaxis of peripheral monocytes. Consistent with our findings, a multicenter, prospective cohort study showed an increased activation of the innate immune system in HBV-ACLF[2]. Immunofluorescence further confirmed that circulating monocyte-derived macrophages widely infiltrated the liver of patients with HBV-ACLF. Moreover, extensive ductular reactions (DR) were noted around the necrotic zone of the liver and around portal areas. DR is pathologically recognized as bile duct hyperplasia and is associated with trans-differentiation of hepatocytes. DR may play an important role in hepatic regeneration[25], though it does not exist in all hepatobiliary diseases. Extracellular matrix, inflammatory cell infiltration, and activated myofibroblasts are also involved in the pathogenesis of DR[26-28]. This implies that DR is closely associated with liver regeneration after severe or prolonged injury.

Mitochondria, which are the main oxygen consumers in cells, are the primary organelles that are affected by hypoxia. In this study, hypoxia significantly changed the ultrastructure of mitochondria as evidenced by mitochondrial swelling and ridge destruction. The number of mitochondria increases as an adaptive response to chronic non-specific cellular damage. FGF21 and GDF15 levels were also determined as biomarkers for the severity of mitochondrial dysfunction. For the first time, a reduction in FGF21 levels was noted in patients with HBV-ACLF. FGF21 and GDF15 levels increase in patients with ACLF as independent predictors of adverse clinical events[6,14]. It's important to note that these data were obtained from peripheral blood.

FGF21 levels may be affected by mitochondrial dysfunction in other damaged organs. A series of different models demonstrated that FGF21 has differential tissue-specific effects and might be a modulator of stress signaling in mild-to-moderate mitochondrial dysfunction. However, the effects of FGF21 are dispensable in severe mitochondrial dysfunction [8]. FGF21 is mainly synthesized and secreted by hepatocytes. Decreased FGF21 levels may be attributed to hepatic

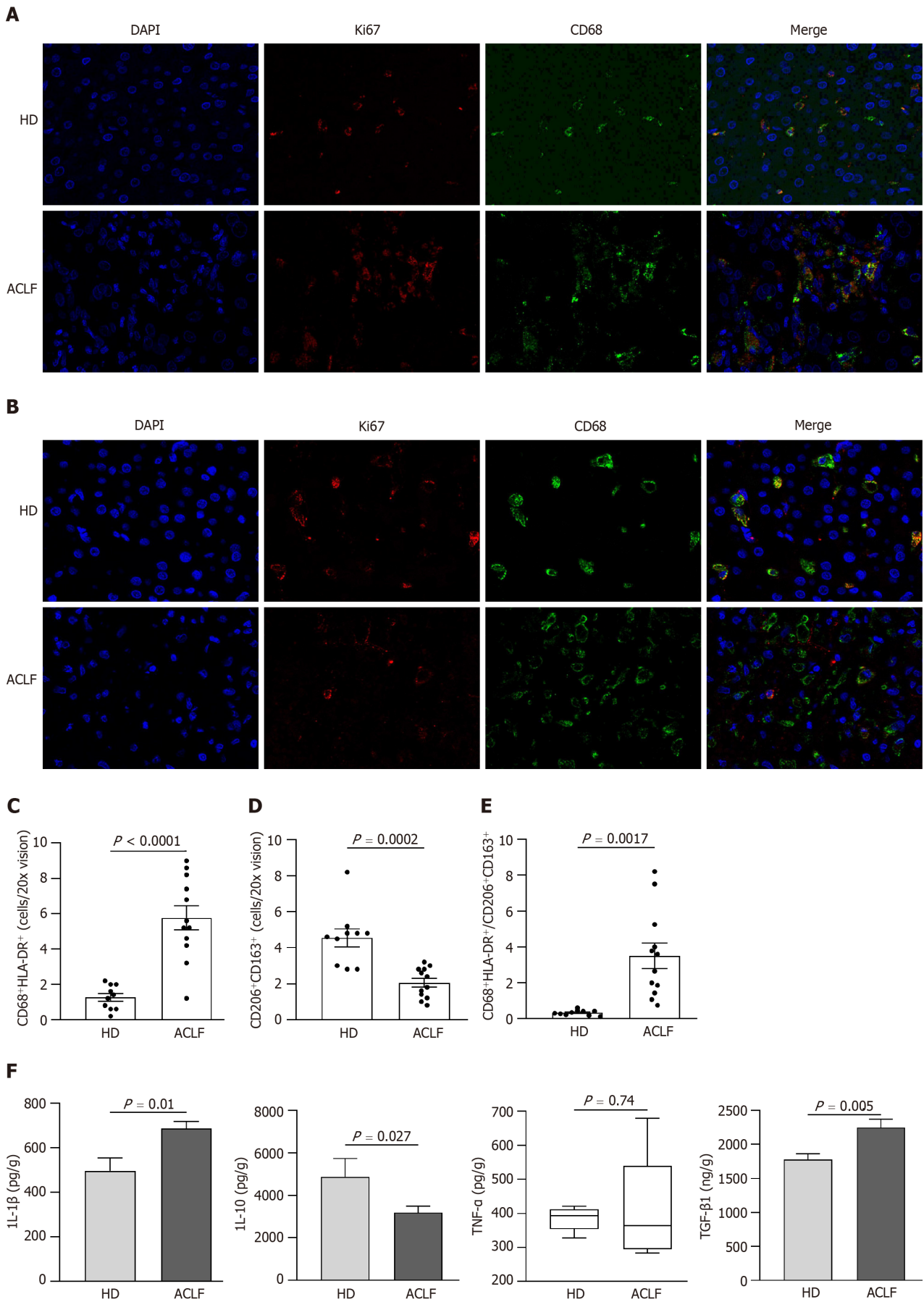


Figure 6 Generalized macrophages activation showed a classically activated phenotype in the liver of patients with acute-on-chronic liver failure. A: Representative microscopic images of double immunofluorescence staining of CD68 and HLA-DR in the liver (400 fold). The red fluorescence signal

represented CD68; the green fluorescence signal represented HLA-DR; and the blue fluorescence signal represented DAPI; B: Representative microscopic images of the double immunofluorescence staining of CD206 and CD163 in the liver (400 fold). The red fluorescence signal represented CD206; the green fluorescence signal represented CD163; and the blue fluorescence signal represented DAPI; C: The mean number of CD68⁺ HLA-DR⁺-positive cells in five × 200 fields; D: The mean number of CD206⁺ CD163⁺-positive cells in five × 200 fields; E: The ratio of CD68⁺ HLA-DR⁺/CD206⁺ CD163⁺-positive cells in healthy donors and patients with acute-on-chronic liver failure; F: The levels of macrophage-derived cytokines (interleukin-1 β , tumor necrosis factor- α , interleukin-10, and transforming growth factor- β 1) in liver homogenates. Data with normal distribution were compared using unpaired student's *t*-test, and the Mann-Whitney test was used for non-normal data. ACLF: Acute-on-chronic liver failure; HD: Healthy donor; IL-1 β : Interleukin-1 β ; IL-10: Interleukin-10; TNF- α : Tumor necrosis factor- α ; TGF- β 1: Transforming growth factor.

insufficiency and massive hepatocyte necrosis in patients with ACLF. GDF15 is a protein that is mainly secreted by activated macrophages[29]. The extensive hepatic infiltration of inflammatory cells was consistent with increased levels of GDF15. A meta-analysis showed that GDF15, which is a biomarker of mitochondrial dysfunction, has higher diagnostic accuracy than FGF21[30]. In conclusion, the FGF21 Levels in the serum do not have diagnostic and prognostic significance in patients with advanced HBV-ACLF. More studies are needed to carefully assess the role of serum biomarkers in predicting serious adverse events in patients with ACLF.

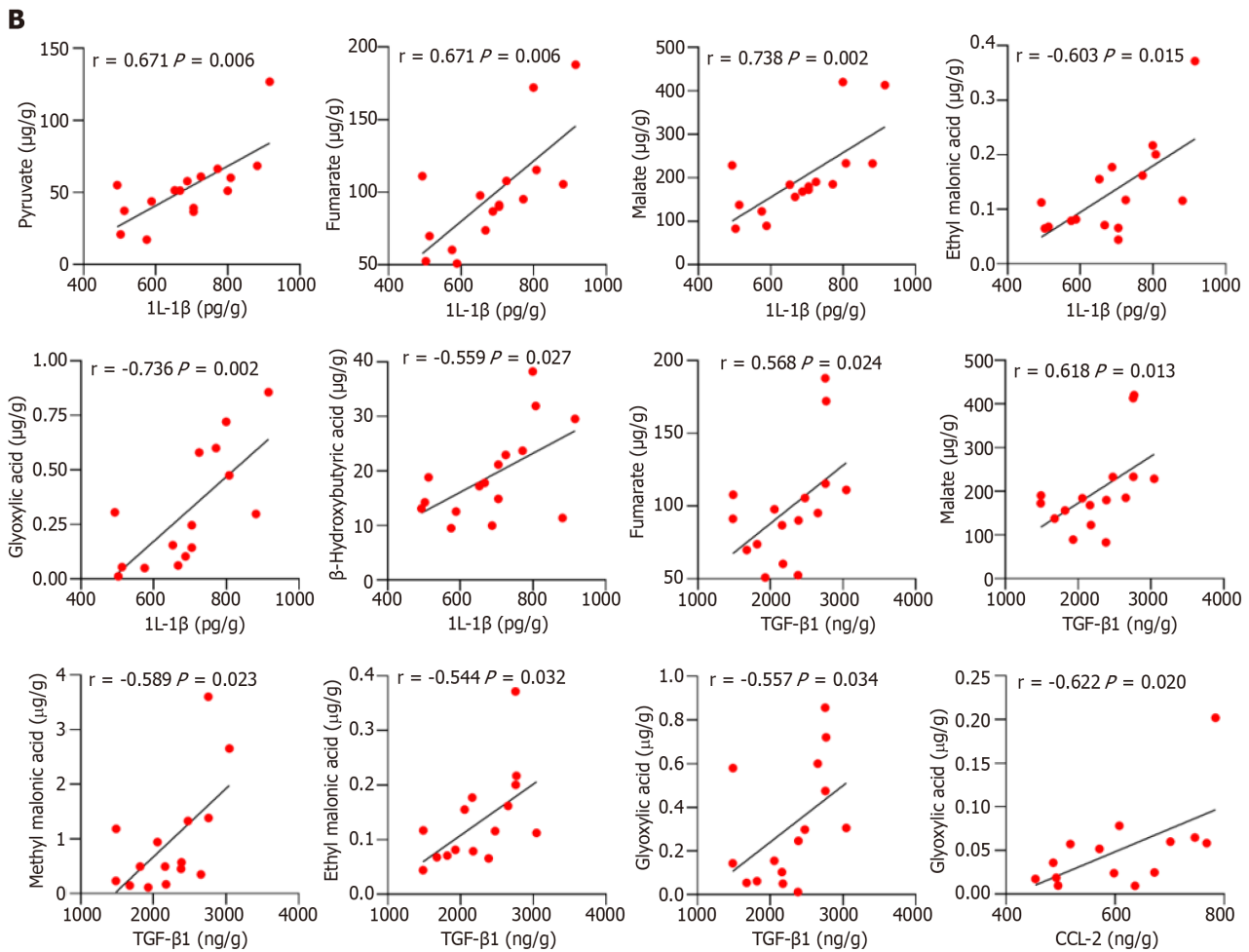
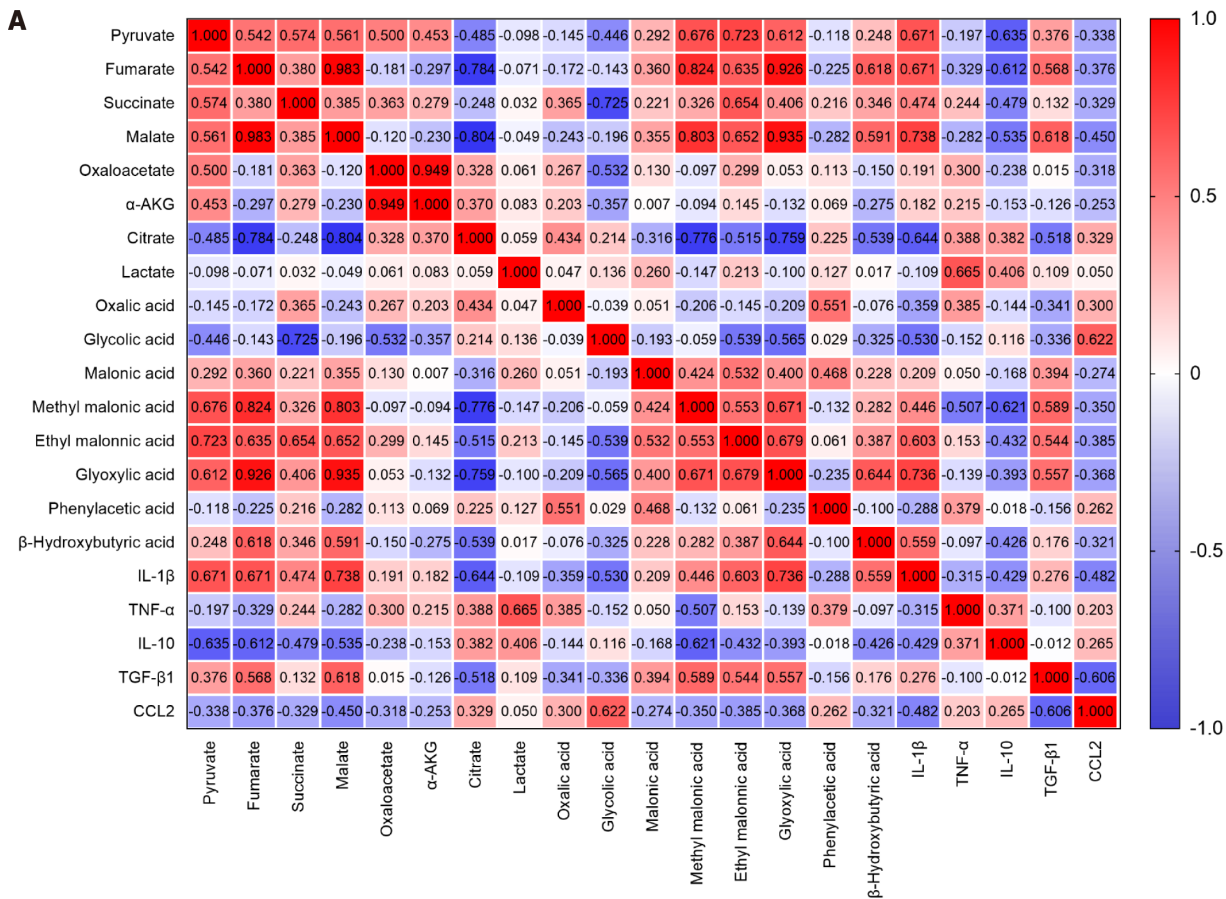
Mitochondrial dysfunction in ACLF severely impairs ATP production so the liver of patients with ACLF provides more energy *via* glycolysis[4]. Decreased fumarate levels and increased succinate levels may be attributed to the inhibition of the TCA cycle. Selective impairments were observed in the conversion of succinate into fumarate in the TCA cycle of leukocytes obtained from patients with ACLF[4]. Similar impairments were observed between isocitric acid and α -ketoglutaric acid[4], and α -ketoglutaric acid accumulation may be due to glutamine supplementation[3]. These results illuminate the metabolic characteristics of the liver of patients with ACLF. These characteristics include enhanced glycolysis and glutamine anaplerosis, inhibited oxidative phosphorylation, and TCA cycle disruption. In contrast, another clinical study found that glycolysis was repressed in the liver of patients with HBV-ACLF[3]. In the same study, patients with ACLF were only admitted to combined medicine. The severity and clinical characteristics of patients were different from those of patients with advanced HBV-ACLF. We hypothesized that glycolysis undergoes a dynamic transition during HBV-ACLF progression. In addition, enhanced glycolysis may not be only a passive transition after mitochondrial dysfunction but also an active choice in hypoxia. In hypoxic conditions, stably expressed HIF-1 α mediates glucose metabolism reprogramming *via* multiple pathways, thereby transforming energy production from oxidative phosphorylation to glycolysis. For example, HIF-1 α increases glucose conversion into LAC by increasing the expression of glucose transporters and glycolytic enzymes[31,32]. HIF-1 α decreases mitochondrial oxidation and promotes glycolysis in macrophages[33].

Macrophage activation is characterized by pronounced metabolic adaptation. Classically activated macrophages secrete proinflammatory mediators. A shift from impaired TCA cycle and oxidative phosphorylation to glycolysis also takes place. In contrast, alternatively activated macrophages secrete anti-inflammatory cytokines and are characterized by enhanced oxidative phosphorylation and fatty acid oxidation[34]. Notably, organic acid metabolites strongly correlated with macrophage-derived cytokines/chemokines, linking metabolism to immunity in ACLF. This study was not designed to elucidate whether metabolic remodeling is the underlying cause or the consequence of immune activation, but there is enough evidence supporting that impaired TCA cycle and enhanced glycolysis reinforce inflammatory responses. High levels of succinate in cells have been shown to stabilize and activate the HIF-1 α and its downstream targets by inhibiting prolyl hydroxylases. This pathway induces IL-1 β secretion in macrophages[35,36]. Accelerated glycolysis may guarantee a competitive bioenergetic state and provide energy for classically activated macrophages to release proinflammatory cytokines[37]. We demonstrated that imbalanced macrophage polarization existed in the pathogenesis of HBV-ACLF. Classically activated macrophages release high amounts of cytokines, leading to tissue damage and organ failure. It can be a new immunometabolic therapeutic strategy to regulate macrophage polarization by inhibiting the glycolysis pathway.

In summary, our findings provided direct mechanistic evidence of tissue hypoxia, mitochondrial dysfunction, metabolic remodeling, and imbalanced immune homeostasis in patients with advanced HBV-ACLF. The interaction between these pathophysiological mechanisms forms an interconnected complex network. HIF-1 α may be the core target in this network. Regulating liver metabolism reprogramming and promoting the polarization of alternatively activated macrophages may attenuate liver inflammation and promote tissue repair. This provides insights to treatment strategies that are worth exploring.

CONCLUSION

The results indicated that bioenergetic alteration driven by hypoxia and mitochondrial dysfunction affects hepatic immune and metabolic remodeling, leading to advanced HBV-ACLF. These findings highlight a new therapeutic target for improving the treatment of HBV-ACLF.



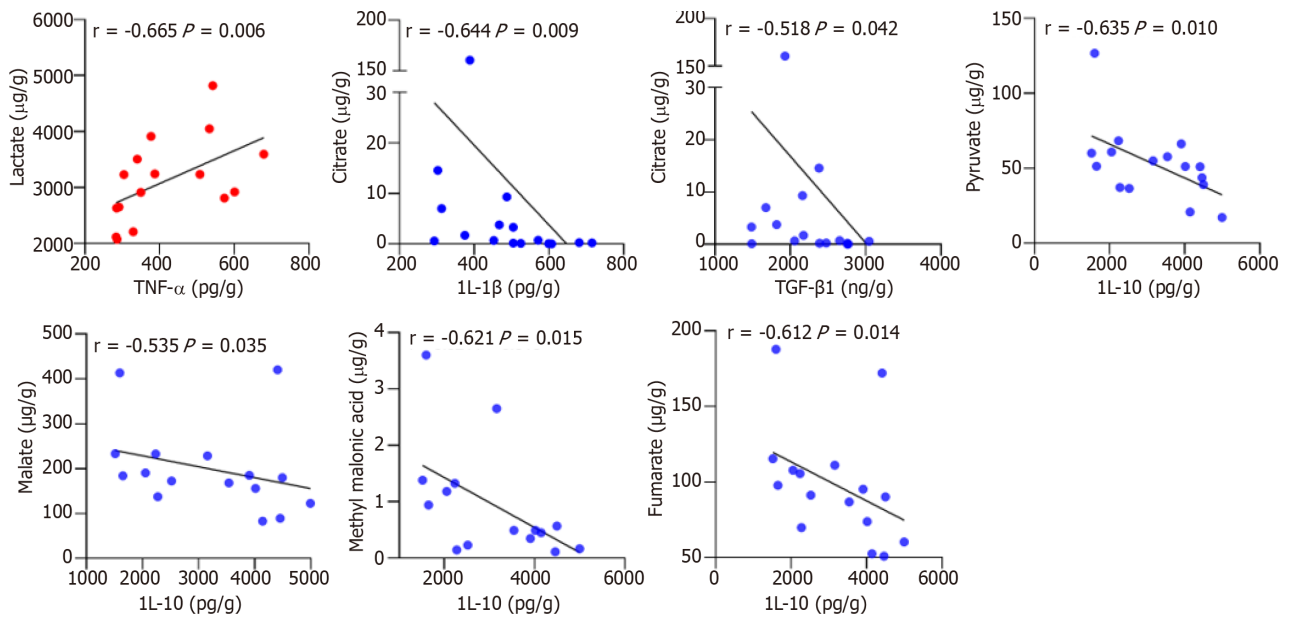


Figure 7 Correlation plot between the 16 organic acid metabolites and macrophage-derived cytokines/chemokines in patients with acute-on-chronic liver failure ($n = 17$). A: Correlation plot between the 16 organic acid metabolites and cytokines/chemokines; B: Linear correlation scatter plot between the organic acid metabolites and cytokines/chemokines ($P < 0.05$). The Spearman test was used to measure the correlations of non-normally distributed variables. IL-1 β : Interleukin-1 β ; IL-10: Interleukin-10; TNF- α : Tumor necrosis factor- α ; TGF- β 1: Transforming growth factor. CCL-2: Chemokine C-C motif ligand 2.

ARTICLE HIGHLIGHTS

Research background

Immune dysregulation and metabolic derangement have been recognized as key factors that contribute to the progression of hepatitis B virus (HBV)-related acute-on-chronic liver failure (ACLF).

Research motivation

Currently, the mechanisms underlying immune and metabolic derangement in patients with advanced HBV-ACLF are unclear.

Research objectives

To identify the bioenergetic alterations in the liver of patients with HBV-ACLF causing hepatic immune dysregulation and metabolic disorders.

Research methods

This study evaluated the mitochondrial ultrastructure, metabolic characteristics, and immune microenvironment of the liver of the subjects.

Research results

There was extensive hepatocyte necrosis, immune cell infiltration, and ductular reaction in the liver of patients with ALCF. Hypoxia significantly changed the ultrastructure of mitochondria as evidenced by mitochondrial swelling and ridge destruction. Mitochondrial oxidative phosphorylation decreased, while anaerobic glycolysis was enhanced in patients with HBV-ACLF. Circulating monocyte-derived macrophages widely infiltrated the liver of patients with HBV-ACLF. Patients with ALCF had a high abundance of CD68⁺ HLA-DR⁺ macrophages and elevated levels of both interleukin-1 β and transforming growth factor- β 1 in their livers. The abundance of CD206⁺ CD163⁺ macrophages and expression of interleukin-10 decreased.

Research conclusions

Bioenergetic alteration driven by hypoxia and mitochondrial dysfunction affects hepatic immune and metabolic remodeling, leading to advanced HBV-ACLF.

Research perspectives

Regulating liver metabolism reprogramming and promoting the polarization of alternatively activated macrophages may attenuate liver inflammation and promote tissue repair. This provides insights to treatment strategies that are worth exploring.

FOOTNOTES

Author contributions: Zhang Y and Tian XL performed experiments, analysed data and wrote the paper; Wu DS and Li Q performed experiments and analysed data; Li JQ and Chen B designed experiments, performed experiments and edited the paper.

Supported by the Domestic First-class Construction Disciplines of the Hunan University of Chinese Medicine; Postgraduate Research Innovation Program of Hunan Province, No. CX20220771; and Clinical MedTech Innovation Project of Hunan Province, No. 2021SK51415.

Institutional review board statement: The study protocol was approved by the Ethics Committee of the First Hospital of Hunan University of Chinese Medicine (No. HN-LL-SWST-15), and written informed consent was obtained from all participants.

Informed consent statement: All study participants, or their legal guardian, provided informed written consent prior to study enrollment.

Conflict-of-interest statement: The authors declare no conflicts of interest that pertain to this work.

Data sharing statement: All data generated or analyzed during this study are included in this published article.

STROBE statement: The authors have read the STROBE Statement – checklist of items, and the manuscript was prepared and revised according to the STROBE Statement – checklist of items.

Open-Access: This article is an open-access article that was selected by an in-house editor and fully peer-reviewed by external reviewers. It is distributed in accordance with the Creative Commons Attribution NonCommercial (CC BY-NC 4.0) license, which permits others to distribute, remix, adapt, build upon this work non-commercially, and license their derivative works on different terms, provided the original work is properly cited and the use is non-commercial. See: <https://creativecommons.org/licenses/by-nc/4.0/>

Country/Territory of origin: China

ORCID number: Yu Zhang 0000-0002-1692-6698; Dong-Sheng Wu 0000-0001-7137-7954; Bin Chen 0000-0002-5485-2263.

S-Editor: Lin C

L-Editor: A

P-Editor: Zhao YQ

REFERENCES

- 1 Sarin SK, Choudhury A, Sharma MK, Maiwall R, Al Mahtab M, Rahman S, Saigal S, Saraf N, Soin AS, Devarbhavi H, Kim DJ, Dhiman RK, Duseja A, Taneja S, Eapen CE, Goel A, Ning Q, Chen T, Ma K, Duan Z, Yu C, Treeprasertsuk S, Hamid SS, Butt AS, Jafri W, Shukla A, Saraswat V, Tan SS, Sood A, Midha V, Goyal O, Ghazinyan H, Arora A, Hu J, Sahu M, Rao PN, Lee GH, Lim SG, Lesmana LA, Lesmana CR, Shah S, Prasad VGM, Payawal DA, Abbas Z, Dokmeci AK, Sollano JD, Carpio G, Shresta A, Lau GK, Fazal Karim M, Shiha G, Gani R, Kalista KF, Yuen MF, Alam S, Khanna R, Sood V, Lal BB, Pamecha V, Jindal A, Rajan V, Arora V, Yokosuka O, Niriella MA, Li H, Qi X, Tanaka A, Mochida S, Chaudhuri DR, Gane E, Win KM, Chen WT, Rela M, Kapoor D, Rastogi A, Kale P, Sharma CB, Bajpai M, Singh V, Premkumar M, Maharashi S, Olithselvan A, Philips CA, Srivastava A, Yachha SK, Wani ZA, Thapa BR, Saraya A, Shalimar, Kumar A, Wadhawan M, Gupta S, Madan K, Sakhuja P, Vij V, Sharma BC, Garg H, Garg V, Kalal C, Anand L, Vyas T, Mathur RP, Kumar G, Jain P, Pasupuleti SSR, Chawla YK, Chowdhury A, Song DS, Yang JM, Yoon EL; APASL ACLF Research Consortium (AARC) for APASL ACLF working Party. Acute-on-chronic liver failure: consensus recommendations of the Asian Pacific association for the study of the liver (APASL): an update. *Hepatology* 2019; **13**: 353-390 [PMID: 31172417 DOI: 10.1007/s12072-019-09946-3]
- 2 Li J, Liang X, Jiang J, Yang L, Xin J, Shi D, Lu Y, Li J, Ren K, Hassan HM, Zhang J, Chen P, Yao H, Wu T, Jin L, Ye P, Li T, Zhang H, Sun S, Guo B, Zhou X, Cai Q, Chen J, Xu X, Huang J, Hao S, He J, Xin S, Wang D, Trebicka J, Chen X; Chinese Group on the Study of Severe Hepatitis B (COSSH). PBMC transcriptomics identifies immune-metabolism disorder during the development of HBV-ACLF. *Gut* 2022; **71**: 163-175 [PMID: 33431576 DOI: 10.1136/gutjnl-2020-323395]
- 3 Yu Z, Li J, Ren Z, Sun R, Zhou Y, Zhang Q, Wang Q, Cui G, Li A, Duan Z, Xu Y, Wang Z, Yin P, Piao H, Lv J, Liu X, Wang Y, Fang M, Zhuang Z, Xu G, Kan Q. Switching from Fatty Acid Oxidation to Glycolysis Improves the Outcome of Acute-On-Chronic Liver Failure. *Adv Sci (Weinh)* 2020; **7**: 1902996 [PMID: 32274306 DOI: 10.1002/advs.201902996]
- 4 Zhang IW, Curto A, López-Vicario C, Casulleras M, Duran-Güell M, Flores-Costa R, Colsch B, Aguilar F, Aransay AM, Lozano JJ, Hernández-Tejero M, Toapanta D, Fernández J, Arroyo V, Clària J. Mitochondrial dysfunction governs immunometabolism in leukocytes of patients with acute-on-chronic liver failure. *J Hepatol* 2022; **76**: 93-106 [PMID: 34450236 DOI: 10.1016/j.jhep.2021.08.009]
- 5 Liver Failure and Artificial Liver Group, Chinese Society of Infectious Diseases; Chinese Medical Association; Severe Liver Disease and Artificial Liver Group, Chinese Society of Hepatology, Chinese Medical Association. [Guideline for diagnosis and treatment of liver failure]. *Zhonghua Gan Zang Bing Za Zhi* 2019; **27**: 18-26 [PMID: 30685919 DOI: 10.3760/cma.j.issn.1007-3418.2019.01.006]
- 6 Schofield CJ, Ratcliffe PJ. Signalling hypoxia by HIF hydroxylases. *Biochem Biophys Res Commun* 2005; **338**: 617-626 [PMID: 16139242 DOI: 10.1016/j.bbrc.2005.08.111]
- 7 Riley LG, Nafisinia M, Menezes MJ, Nambiar R, Williams A, Barnes EH, Selvanathan A, Lichkus K, Bratkovic D, Yaplitto-Lee J, Bhattacharya K, Ellaway C, Kava M, Balasubramaniam S, Christodoulou J. FGF21 outperforms GDF15 as a diagnostic biomarker of mitochondrial disease in children. *Mol Genet Metab* 2022; **135**: 63-71 [PMID: 34991945 DOI: 10.1016/j.ymgme.2021.12.001]

- 8 **Croon M**, Szczepanowska K, Popovic M, Lienkamp C, Senft K, Brandscheid CP, Bock T, Gnatzy-Feik L, Ashurov A, Acton RJ, Kaul H, Pujol C, Rosenkranz S, Krüger M, Trifunovic A. FGF21 modulates mitochondrial stress response in cardiomyocytes only under mild mitochondrial dysfunction. *Sci Adv* 2022; **8**: eabn7105 [PMID: 35385313 DOI: 10.1126/sciadv.abn7105]
- 9 **Lehtonen JM**, Forsström S, Bottani E, Viscomi C, Baris OR, Isoniemi H, Höckerstedt K, Österlund P, Hurme M, Jylhävä J, Leppä S, Markkula R, Heliö T, Mombelli G, Uusimaa J, Laaksonen R, Laaksovirta H, Auranen M, Zeviani M, Smeitink J, Wiesner RJ, Nakada K, Isohanni P, Suomalainen A. FGF21 is a biomarker for mitochondrial translation and mtDNA maintenance disorders. *Neurology* 2016; **87**: 2290-2299 [PMID: 27794108 DOI: 10.1212/WNL.0000000000003374]
- 10 **Wu L**, Pan Q, Wu G, Qian L, Zhang J, Zhang L, Fang Q, Zang G, Wang Y, Lau G, Li H, Jia W. Diverse Changes of Circulating Fibroblast Growth Factor 21 Levels in Hepatitis B Virus-Related Diseases. *Sci Rep* 2017; **7**: 16482 [PMID: 29184085 DOI: 10.1038/s41598-017-16312-6]
- 11 **Ruiz-Margáin A**, Pohlmann A, Ryan P, Schierwagen R, Chi-Cervera LA, Jansen C, Mendez-Guerrero O, Flores-García NC, Lehmann J, Torre A, Macías-Rodríguez RU, Trebicka J. Fibroblast growth factor 21 is an early predictor of acute-on-chronic liver failure in critically ill patients with cirrhosis. *Liver Transpl* 2018; **24**: 595-605 [PMID: 29476704 DOI: 10.1002/lt.25041]
- 12 **Wu G**, Wu S, Yan J, Gao S, Zhu J, Yue M, Li Z, Tan X. Fibroblast Growth Factor 21 Predicts Short-Term Prognosis in Patients With Acute Heart Failure: A Prospective Cohort Study. *Front Cardiovasc Med* 2022; **9**: 834967 [PMID: 35369322 DOI: 10.3389/fcvm.2022.834967]
- 13 **Gu L**, Jiang W, Xu Z, Li W, Zhang H. Elevated serum FGF21 levels predict heart failure during hospitalization of STEMI patients after emergency percutaneous coronary intervention. *PeerJ* 2023; **11**: e14855 [PMID: 36778154 DOI: 10.7717/peerj.14855]
- 14 **Fujita Y**, Ito M, Ohsawa I. Mitochondrial stress and GDF15 in the pathophysiology of sepsis. *Arch Biochem Biophys* 2020; **696**: 108668 [PMID: 33188737 DOI: 10.1016/j.abb.2020.108668]
- 15 **Li H**, Tang D, Chen J, Hu Y, Cai X, Zhang P. The Clinical Value of GDF15 and Its Prospective Mechanism in Sepsis. *Front Immunol* 2021; **12**: 710977 [PMID: 34566964 DOI: 10.3389/fimmu.2021.710977]
- 16 **Lin Y**, Wang Y, Li PF. Mutual regulation of lactate dehydrogenase and redox robustness. *Front Physiol* 2022; **13**: 1038421 [PMID: 36407005 DOI: 10.3389/fphys.2022.1038421]
- 17 **Mehla K**, Singh PK. Metabolic Regulation of Macrophage Polarization in Cancer. *Trends Cancer* 2019; **5**: 822-834 [PMID: 31813459 DOI: 10.1016/j.trecan.2019.10.007]
- 18 **de Goede KE**, Harber KJ, Gorki FS, Verberk SGS, Groh LA, Keuning ED, Struys EA, van Weeghel M, Haschemi A, de Winther MPJ, van Dierendonck XAMH, Van den Bossche J. d-2-Hydroxyglutarate is an anti-inflammatory immunometabolite that accumulates in macrophages after TLR4 activation. *Biochim Biophys Acta Mol Basis Dis* 2022; **1868**: 166427 [PMID: 35526742 DOI: 10.1016/j.bbadis.2022.166427]
- 19 **He W**, Miao FJ, Lin DC, Schwandner RT, Wang Z, Gao J, Chen JL, Tian H, Ling L. Citric acid cycle intermediates as ligands for orphan G-protein-coupled receptors. *Nature* 2004; **429**: 188-193 [PMID: 15141213 DOI: 10.1038/nature02488]
- 20 **Rubic T**, Lametschwandner G, Jost S, Hinteregger S, Kund J, Carballido-Perrig N, Schwärzler C, Junt T, Voshol H, Meingassner JG, Mao X, Werner G, Rot A, Carballido JM. Triggering the succinate receptor GPR91 on dendritic cells enhances immunity. *Nat Immunol* 2008; **9**: 1261-1269 [PMID: 18820681 DOI: 10.1038/ni.1657]
- 21 **Eltzschig HK**, Carmeliet P. Hypoxia and inflammation. *N Engl J Med* 2011; **364**: 656-665 [PMID: 21323543 DOI: 10.1056/NEJMra0910283]
- 22 **Chen L**, Huang L, Gu Y, Cang W, Sun P, Xiang Y. Lactate-Lactylation Hands between Metabolic Reprogramming and Immunosuppression. *Int J Mol Sci* 2022; **23** [PMID: 36233246 DOI: 10.3390/ijms231911943]
- 23 **Semba H**, Takeda N, Isagawa T, Sugiura Y, Honda K, Wake M, Miyazawa H, Yamaguchi Y, Miura M, Jenkins DM, Choi H, Kim JW, Asagiri M, Cowburn AS, Abe H, Soma K, Koyama K, Katoh M, Sayama K, Goda N, Johnson RS, Manabe I, Nagai R, Komuro I. HIF-1 α -PDK1 axis-induced active glycolysis plays an essential role in macrophage migratory capacity. *Nat Commun* 2016; **7**: 11635 [PMID: 27189088 DOI: 10.1038/ncomms11635]
- 24 **Moreau R**, Clària J, Aguilar F, Fenaille F, Lozano JJ, Junot C, Colsch B, Caraceni P, Trebicka J, Pavesi M, Alessandria C, Nevens F, Saliba F, Welzel TM, Albillos A, Gustot T, Fernández J, Moreno C, Baldassarre M, Zaccherini G, Piano S, Montagnese S, Vargas V, Genescà J, Solà E, Bernal W, Butin N, Hautbergue T, Cholet S, Castelli F, Jansen C, Steib C, Campion D, Mookerjee R, Rodríguez-Gandía M, Soriano G, Durand F, Bente D, Bañares R, Stauber RE, Gronbaek H, Coenraad MJ, Ginès P, Gerbes A, Jalan R, Bernardi M, Arroyo V, Angeli P; CANONIC Study Investigators of the EASL Clif Consortium; Grifols Chair; European Foundation for the Study of Chronic Liver Failure (EF Clif). Blood metabolomics uncovers inflammation-associated mitochondrial dysfunction as a potential mechanism underlying ACLF. *J Hepatol* 2020; **72**: 688-701 [PMID: 31778751 DOI: 10.1016/j.jhep.2019.11.009]
- 25 **Sato K**, Marzioni M, Meng F, Francis H, Glaser S, Alpini G. Ductular Reaction in Liver Diseases: Pathological Mechanisms and Translational Significances. *Hepatology* 2019; **69**: 420-430 [PMID: 30070383 DOI: 10.1002/hep.30150]
- 26 **Roskams TA**, Theise ND, Balabaud C, Bhagat G, Bhatnath PS, Bioulac-Sage P, Brunt EM, Crawford JM, Crosby HA, Desmet V, Finegold MJ, Geller SA, Gouw AS, Hytiroglou P, Knisely AS, Kojiro M, Lefkowitz JH, Nakanuma H, Olynyk JK, Park YN, Portmann B, Saxena R, Scheuer PJ, Strain AJ, Thung SN, Wanless IR, West AB. Nomenclature of the finer branches of the biliary tree: canals, ductules, and ductular reactions in human livers. *Hepatology* 2004; **39**: 1739-1745 [PMID: 15185318 DOI: 10.1002/hep.20130]
- 27 **Gadd VL**, Skoien R, Powell EE, Fagan KJ, Winterford C, Horsfall L, Irvine K, Clouston AD. The portal inflammatory infiltrate and ductular reaction in human nonalcoholic fatty liver disease. *Hepatology* 2014; **59**: 1393-1405 [PMID: 24254368 DOI: 10.1002/hep.26937]
- 28 **Lorenzini S**, Bird TG, Boulter L, Bellamy C, Samuel K, Aucott R, Clayton E, Andreone P, Bernardi M, Golding M, Alison MR, Iredale JP, Forbes SJ. Characterisation of a stereotypical cellular and extracellular adult liver progenitor cell niche in rodents and diseased human liver. *Gut* 2010; **59**: 645-654 [PMID: 20427399 DOI: 10.1136/gut.2009.182345]
- 29 **Wollert KC**, Kempf T, Wallentin L. Growth Differentiation Factor 15 as a Biomarker in Cardiovascular Disease. *Clin Chem* 2017; **63**: 140-151 [PMID: 28062617 DOI: 10.1373/clinchem.2016.255174]
- 30 **Lin Y**, Ji K, Ma X, Liu S, Li W, Zhao Y, Yan C. Accuracy of FGF-21 and GDF-15 for the diagnosis of mitochondrial disorders: A meta-analysis. *Ann Clin Transl Neurol* 2020; **7**: 1204-1213 [PMID: 32585080 DOI: 10.1002/acn3.51104]
- 31 **Semenza GL**. Hypoxia-inducible factor 1: regulator of mitochondrial metabolism and mediator of ischemic preconditioning. *Biochim Biophys Acta* 2011; **1813**: 1263-1268 [PMID: 20732359 DOI: 10.1016/j.bbamer.2010.08.006]
- 32 **Semenza GL**. HIF-1: upstream and downstream of cancer metabolism. *Curr Opin Genet Dev* 2010; **20**: 51-56 [PMID: 19942427 DOI: 10.1016/j.gde.2009.10.009]
- 33 **Wang T**, Liu H, Lian G, Zhang SY, Wang X, Jiang C. HIF1 α -Induced Glycolysis Metabolism Is Essential to the Activation of Inflammatory Macrophages. *Mediators Inflamm* 2017; **2017**: 9029327 [PMID: 29386753 DOI: 10.1155/2017/9029327]

- 34 **Liu Y**, Xu R, Gu H, Zhang E, Qu J, Cao W, Huang X, Yan H, He J, Cai Z. Metabolic reprogramming in macrophage responses. *Biomark Res* 2021; **9**: 1 [PMID: 33407885 DOI: 10.1186/s40364-020-00251-y]
- 35 **Tannahill GM**, Curtis AM, Adamik J, Palsson-McDermott EM, McGettrick AF, Goel G, Frezza C, Bernard NJ, Kelly B, Foley NH, Zheng L, Gardet A, Tong Z, Jany SS, Corr SC, Haneklaus M, Caffrey BE, Pierce K, Walmsley S, Beasley FC, Cummins E, Nizet V, Whyte M, Taylor CT, Lin H, Masters SL, Gottlieb E, Kelly VP, Clish C, Auron PE, Xavier RJ, O'Neill LA. Succinate is an inflammatory signal that induces IL-1 β through HIF-1 α . *Nature* 2013; **496**: 238-242 [PMID: 23535595 DOI: 10.1038/nature11986]
- 36 **Majmudar AJ**, Wong WJ, Simon MC. Hypoxia-inducible factors and the response to hypoxic stress. *Mol Cell* 2010; **40**: 294-309 [PMID: 20965423 DOI: 10.1016/j.molcel.2010.09.022]
- 37 **Freemerman AJ**, Johnson AR, Sacks GN, Milner JJ, Kirk EL, Troester MA, Macintyre AN, Goraksha-Hicks P, Rathmell JC, Makowski L. Metabolic reprogramming of macrophages: glucose transporter 1 (GLUT1)-mediated glucose metabolism drives a proinflammatory phenotype. *J Biol Chem* 2014; **289**: 7884-7896 [PMID: 24492615 DOI: 10.1074/jbc.M113.522037]



Published by **Baishideng Publishing Group Inc**
7041 Koll Center Parkway, Suite 160, Pleasanton, CA 94566, USA
Telephone: +1-925-3991568
E-mail: office@baishideng.com
Help Desk: <https://www.f6publishing.com/helpdesk>
<https://www.wjgnet.com>

